JOURNAL OF GEOPHYSICAL RESEARCH, VOL. 96, NO. B3, PAGES 4457–4478, MARCH 10, 1991

The Collision Zone Between the North d'Entrecasteaux Ridge and the New Hebrides Island Arc 1. Sea Beam Morphology and Shallow Structure

JEAN-YVES COLLOT
Laboratoire de Géodynamique, ORSTOM, Villefranche sur mer, France
MICHAEL A. FISHER
U.S. Geological Survey, Menlo Park, California

Sea Beam bathymetric data, closely spaced single-channel seismic reflection sections, and geopotential field data were collected aboard the R/V *J. Charcot* over the collision zone between the North d'Entrecasteaux Ridge (NDR) and the New Hebrides island arc. The NDR trends east at a small angle (14°) to the plate convergence direction so that the ridge creeps northward along the trench at about 2.5 cm/yr, requiring a continual structural adjustment of the accretionary complex. In this report we study the shallow structure, tectonic erosion, and consequent mass wasting of the accretionary complex, all of which were produced by the collision of the NDR in a complex deformational environment. The accretionary complex in this collision zone can be divided into northern, central, and southern parts. The northern part of the collision zone, which lies north of the leading flank of the ridge, shows a lobate lower accretionary complex that is structured by east to southeast dipping thrust and reverse faults and N60°W trending strike-slip faults; a middle accretionary complex that bulges seaward and appears to be rotated 45°E from the regional arc trend; and an upper accretionary complex that is shaped by slumps and a canyon network. The central part of the collision zone, which directly overlies the crest of the ridge, forms a broad shallow protrusion that is bounded on its northern and southern sides by steep scarps. Rocks forming this protrusion have been uplifted, possibly by as much as 1500-2500 m, and tilted to the north, causing northward block sliding along an extensional detachment surface. The southern part of the collision zone, which lies in the wake of the ridge, is deformed by large slumps and normal faults that trend parallel to the ridge axis. Rocks forming this southern part collapse, causing widespread mass wasting. These geophysical data indicate that normal trench convergence has apparently produced only a few trench-parallel structures confined to the toe of the accretionary complex, whereas the along-trench motion of the NDR has resulted in well-developed structures that extend obliquely across the arc slope and form an asymmetric tectonic pattern. The area of the accretionary complex that is disturbed by collision appears to be about twice as wide as the width of the NDR, and the time required to heal the disturbance may be about 0.8 m.y.

INTRODUCTION

A general model of arc-seamount collision has arisen from the study of several seamounts at different stages of subduction along the Japan trench [*Lallemand and Le Pichon*, 1987]. This model predicts that when a seamount enters the subduction zone, compressive thickening develops at the toe of the margin and is followed by extension and erosion of the margin when the trailing flank of the seamount is subducted. *von Huene and Lallemand* [1990] emphasize the important role played by the subduction of positive oceanic features on the tectonic erosion of convergent margins. However, the tectonic processes and erosional mechanisms that accompany the oblique subduction of a ridge have been poorly documented. An exception is the Louisville ridge that sweeps southward along the Tonga trench and enhances the rate of erosion of the Tongan margin [*Pelletier and Dupont*, 1990; *Ballance et al.*, 1989]. In this study we investigate the structural accommodation of an accretionary complex in response to the slightly oblique subduction of the d'Entrecasteaux zone (DEZ) beneath the New Hebrides island arc.

In the southwest Pacific Ocean, the New Hebrides trench marks the plate boundary along which the Australia-India plate on the west underthrusts the Pacific plate and the North Fiji basin on the east (Figure 1). The d'Entrecasteaux zone, which is carried by the Australia-India plate, is a curvilinear submarine chain that extends from the northern New Caledonia ridge to the central New Hebrides arc (Figure 1). Close to the New Hebrides trench, the d'Entrecasteaux zone comprises the high relief (2-4 km), east trending North d'Entrecasteaux ridge (NDR) and South d'Entrecasteaux chain (SDC) (Figure 1). Both features clog the trench and deform the forearc, and they may have been subducted since about 2 Ma [*Pascal et al.*, 1978; *Carney and Macfarlane*, 1982; *Daniel and Katz*, 1981; *Collot et al.*, 1985, *Fisher et al.*, 1986] (Figure 1). The convergence rate between the Australia-India and Pacific plates is about 10 cm/yr [*Minster and Jordan*, 1978] to the east (N76°E ± 11°) [*Isacks et al.*, 1981]. The east trending DEZ is slightly oblique (14°) to the estimated direction of plate convergence, so that the DEZ creeps slowly northward parallel to the trench at an average rate of about 2.5 cm/yr.

In October 1985, leg 1 of the SEAPSO cruise was jointly conducted aboard the French R/V *J. Charcot* by the Institut Français de Recherche Scientifique pour le Développement en Coopération (ORSTOM) and the Institut Français de Recherche pour l'Exploitation de la Mer (IFREMER). During this cruise, Sea Beam bathymetric data, single-channel seismicreflection profiles and geopotential data were collected over the collision zone between the d'Entrecasteaux zone and the New Hebrides arc [*Daniel et al.*, 1986]. These critical Sea Beam bathymetric data as well as multichannel seismic reflection data collected aboard the R/V *S.P. Lee* by a group of scientists from Australia, New Zealand, France, and the United

Copyright 1991 by the American Geophysical Union.

Paper number 90JB01935.
0148-0227/91/90JB-01935$05.00

O.R.S.T.O.M. Fonds Documentaire
N° : 35501 ex1
NBEX 2 : 1 Cote : B

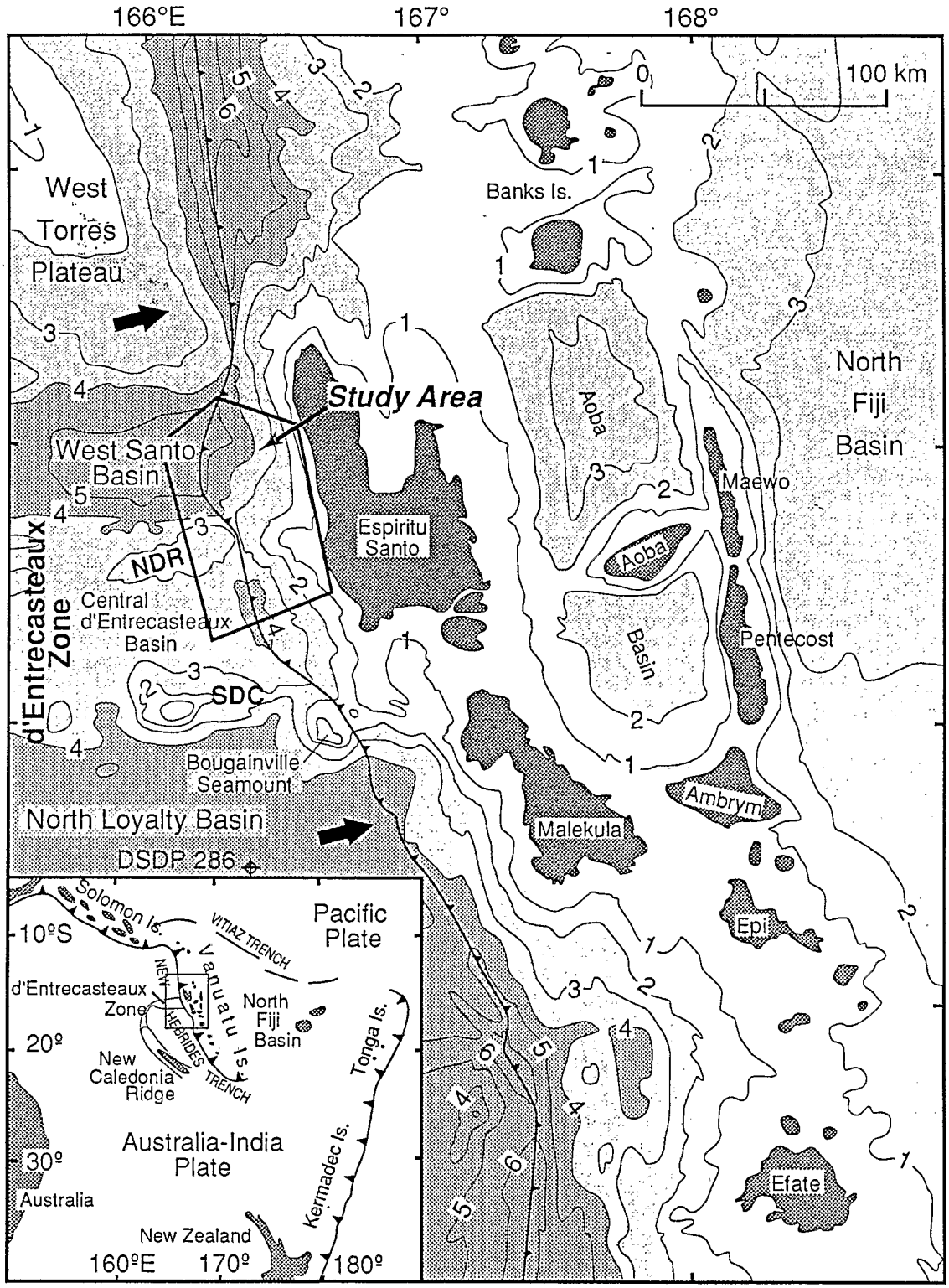

Fig. 1. Location of the study area within the central New Hebrides island arc. Barbed line shows the trace of the interplate decollement, barbs show downdip direction. NDR is North d'Entrecasteaux ridge, SDC is South d'Entrecasteaux chain. Large arrows show the relative motion between the Australia-India and the North Fiji basin plates. Bathymetric contour interval is 1 km.

States form the basis for two complementary studies that concern the collision zones.

This study focuses on the morphology, shallow structure, and erosion of the accretionary complex that were produced by the NDR collision. The companion study [*Fisher et al.*, this issue] deals with the deep structure of this collision zone and the geology of the NDR.

Previous work has shown that the NDR underthrusts the arc slope and deforms the plate boundary. From multichannel seismic reflection data, *Fisher et al.*, [1986] show that the NDR

extends at least 15 km arcward from the trench, below the accretionary complex, and that this collision does not generate large anticlines under the arc slope. Furthermore, new geophysical data reported here provide a more three-dimensional view of the shallow structure than do data presented in earlier reports. In particular, seismic reflection and Sea Beam bathymetric data reveal that, in addition to shortening of the accretionary complex normal to the trench, the dominant deformation caused by the subduction of the NDR includes vigorous uplift of the accretionary complex and strong lateral tectonic movements. These lateral movements produce trenchward bulging of the arc slope [*Collot et al.*, 1985], strike-slip faulting, extensive normal faulting that is transverse to the arc slope, and an intense mass wasting of accreted rocks.

PLATE TECTONIC SETTING OF THE D'ENTRECASTEAUX ZONE

The d'Entrecasteaux zone consists of morphologically distinct western and eastern parts. Close to New Caledonia, the western DEZ encompasses an arcuate elongated graben that is flanked by subparallel horsts, whereas the eastern DEZ widens to the east and includes the North d'Entrecasteaux ridge (NDR) and the South d'Entrecasteaux chain (SDC) (Figure 1).

Dredging indicates that the lithology of the western horsts and of the NDR differ from that of SDC. Latest Paleocene to early Oligocene mid-oceanic ridge basalt were dredged from along the horsts and the NDR [*Maillet et al.*, 1983], whereas dredging of the Bougainville seamount, one of the peaks of the SDC, recovered island arc basalt and andesite as well as middle Eocene to middle Oligocene sedimentary rock.

The North Loyalty and the West Torres basins, under water 4500-5000 m deep, lie astride the DEZ (Figure1). Magnetic anomalies [*Weissel et al.*, 1983] and drilling at Deep Sea Drilling Project (DSDP) site 286 [*Andrews et al.*, 1975] suggest that the North Loyalty basin was an active marginal basin during the late Paleocene to the late Eocene. The age of the West Torres basin is unknown; however, seismic refraction velocities [*Pontoise and Tiffin*, 1986], basement morphology, and sediment characteristics [*Burne et al.*, 1988] all suggest that the crusts of the North Loyalty and the West Torres basins had different origins and that, therefore, the DEZ may be a fossil plate boundary.

Several interpretations have been proposed for the plate tectonic setting of the DEZ. Initially called the d'Entrecasteaux Fracture Zone by *Mallick* [1973] and *Luyendick et al.*, [1974], the DEZ was later interpreted by *Maillet et al.* [1983] as the northern termination of the Eocene subduction/obduction zone that is exposed on New Caledonia. *Maillet et al.*, [1983] proposed that the present morphology of the DEZ resulted from middle Miocene crustal extension. However, during the Eocene, while the North Loyalty basin was active, the eastern DEZ may have been the site of a south dipping subduction zone [Burne et al., 1988]. The trench-like morphology of the basement of the West Santo basin and island-arc affinities of rocks dredged at the Bougainville seamount as well as the Eocene andesite recovered at DSDP site 286 support this interpretation.

REGIONAL GEOLOGIC SETTING OF THE NEW HEBRIDES SUBDUCTION ZONE

The classical arc-trench system developed in the northern and southern parts of the New Hebrides island arc changes greatly in the central part of the arc, where a deep trench is absent [*Karig and Mammerickx*, 1971], where three north trending chains of islands emerge abruptly and replace the single chain present elsewhere, and where the thick sedimentary accumulation within the Aoba basin underlies water 3000 m deep [*Luyendyck et al.*, 1974; *Katz*, 1988; *Fisher et al.*, 1988; *Greene and Johnson*, 1988] (Figure1). Onshore geology suggests that the volcanic foundation of the New Hebrides arc originated during the late Oligocene(?) and early Miocene along a subduction zone that may have faced east and is now represented by the fossil Vitiaz trench [*Carney and Macfarlane*, 1982]. Strong volcanism, which ceased by the end of the middle Miocene, gave rise to the western island chain that includes Espiritu Santo and Malekula Islands. No rocks from the accretionary wedge are exposed on Espiritu Santo Island. Instead, exposed tuffs, pillow lava and volcaniclastic deposits [*Robinson*, 1969; *Mallick and Greenbaum*, 1977] indicate late Oligocene to early Miocene arc volcanism (Figure 2). During the pre-Miocene phase of subduction, the volcanic centers of the western chain probably shed material westward from the islands into what was then a back arc region. These rocks may form part of the basement of the present trenchward slope west of Espiritu Santo and Malekula Islands.

During late Miocene time, at the inception of spreading in the North Fiji Basin [*Malahoff et al.*, 1982], the volcanic axis shifted from the western to the eastern chain that is formed by Pentecost and Maewo Islands (Figure 1). This shift, which may have been caused by a flip of the subduction polarity from east to west facing [*Chase*, 1971; *Falvey*, 1975], correlates in time with uplift and erosion of Espiritu Santo Island. Evidence for erosion is revealed by river valleys that developed in early Miocene rocks and were filled with late Miocene hemipelagic sediments [*Carney et al*, 1985]. We infer that some of the erosional debris now underlies the present trench slope west of Espiritu Santo Island. Because the west facing subduction zone probably began during the late Miocene, the present accretionary complex could have begun to form by the end of the Miocene.

By the early Pliocene, the eastern volcanic chain became inactive and was replaced during the late Pliocene by the present volcanic arc. The forearc area was uplifted during the late Pliocene [*Mallick and Greenbaum*, 1977; *Carney and Macfarlane*, 1980], and uplift accelerated to peak intensity during the Holocene along the western and eastern chains [*Mitchell and Warden*, 1971]. Evidence for the beginning of this uplift is provided on Espiritu Santo Island by a change from hemipelagic deposits to Quaternary fluvial and neritic deposits [*Carney et al.*, 1985]. Furthermore, during the Holocene reef terraces on both Malekula and Espiritu Santo Islands were rapidly uplifted (3.6-6 mm/yr) and tilted eastward [*Taylor et al.*, 1980, 1985, 1987; *Jouannic et al.*, 1980]. This phase of uplift has been interpreted to be a consequence of the onset of the DEZ collision. Such uplift suggests that at least since the late Pliocene, these islands could have been a major source of sediment for the present accretionary complex.

SEISMICITY NEAR THE ARC/DEZ COLLISION

Although on a regional scale the geometry of the Benioff zone beneath the New Hebrides arc dips uniformly at about 70° east, several authors [*Pascal et al.*, 1978; *Chung and Kanamori*, 1978, *Isacks et al.*, 1981; *Marthelot et al.*, 1985; *Louat et al.*, 1988] correlate unusual features of the seismicity in the central New Hebrides arc with the subduction of the DEZ. Among these

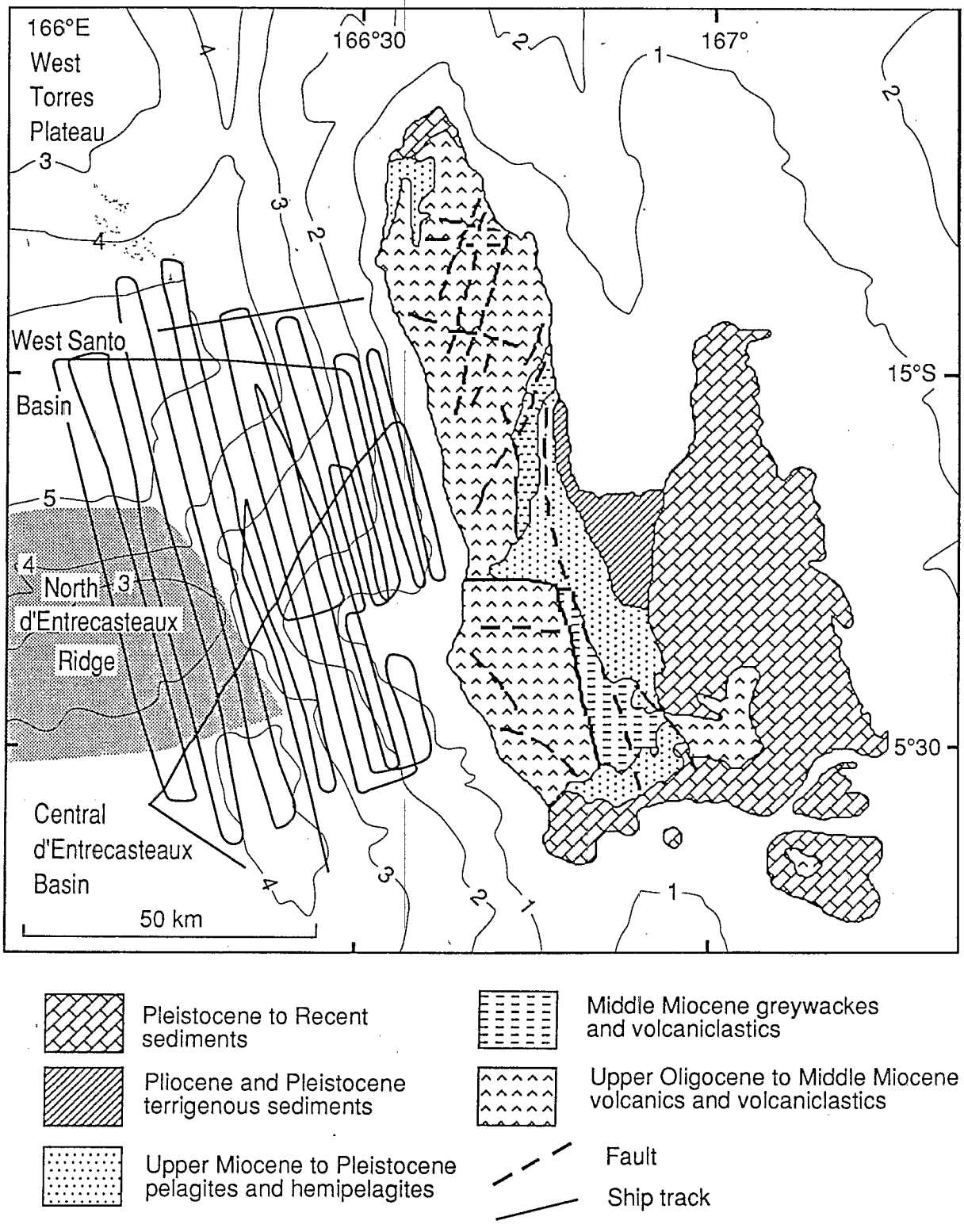

Fig. 2. Simplified geologic map of Espiritu Santo Island and ship tracks of the SEAPSO cruise leg 1 within the surveyed area. None of the exposed rocks represent an accretionary wedge. Bathymetric contour interval is 1 km.

features are a boundary between the aftershock zones of the major 1965 and 1974 shallow earthquakes, which closely corresponds not only with the eastward projection of the NDR [*Isacks et al.*, 1981] but also with a tilt discontinuity in Quaternary reef terraces [*Taylor al.*, 1980]. In addition to a generally less intense seismicity near the DEZ than elsewhere along the arc [*Habermann*, 1984], a remarkable gap in the intermediate-depth seismicity between 100 and 200 km is shown to lie close along the extrapolated location of the subducted part of the DEZ [*Marthelot et al.*, 1985].

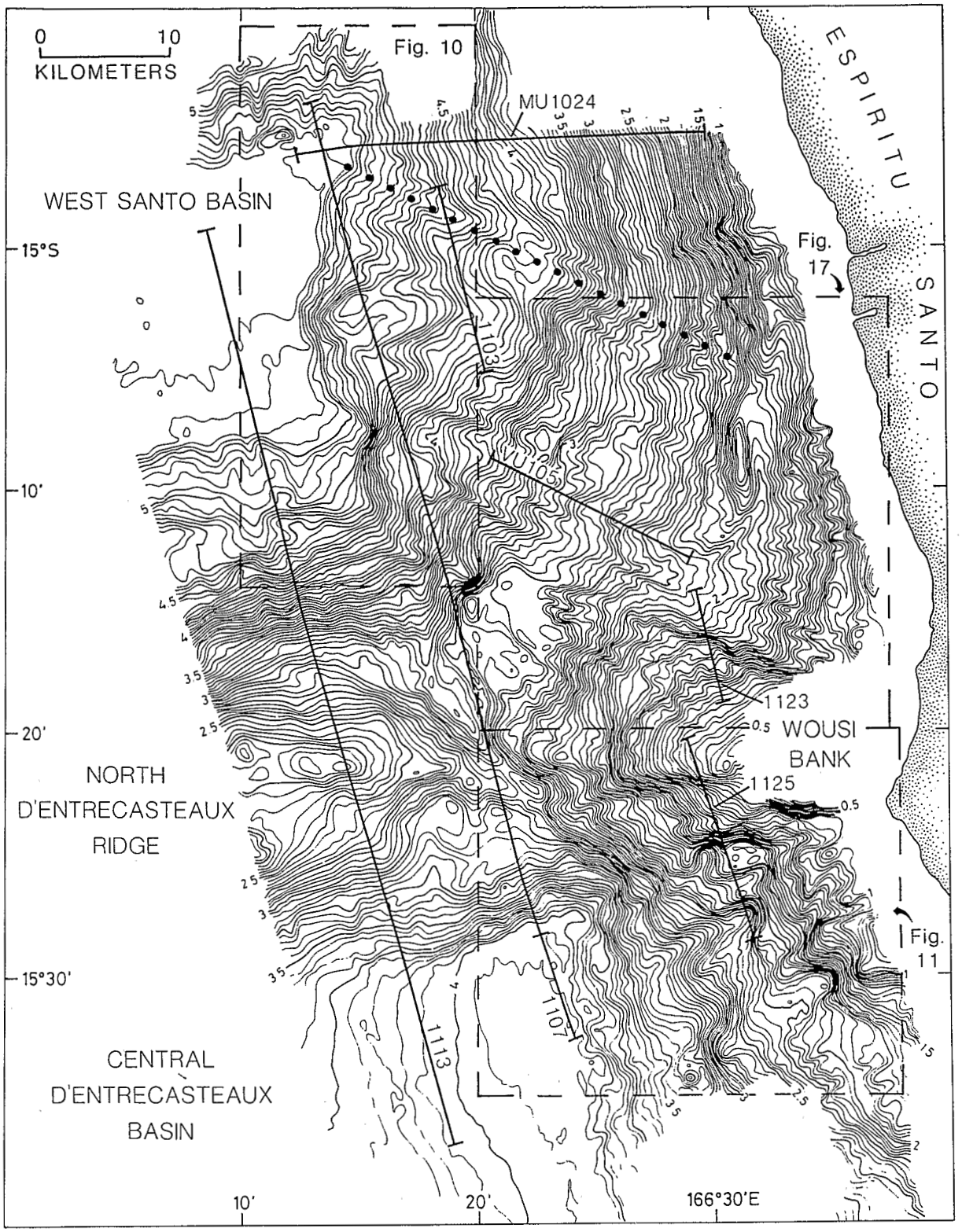

Fig. 3. Generalized Sea Beam bathymetric map of the collision zone between the North d'Entrecasteaux Ridge and the New Hebrides island arc. Contours interval is 50 m. The area covered is shown in Figure 1. Solid dots indicate the northern boundary of the collision zone. Heavy lines refer to seismic sections shown in this report, and dashed boxes outline detailed Sea Beam maps.

GEOPHYSICAL DATA

Detailed geophysical surveys of the collision zone between the NDR and the New Hebrides arc cover about 3600 km^2 (Figure 2). During the SEAPSO cruise, the ship's position was determined by a Transit satellite navigation system that was augmented for 8 hours each day by more accurate positions obtained from Global Positioning System (GPS) satellite data.

Additional Sea Beam data collected during the MULTIPSO cruise of the R. V. *J. Charcot* (May, 1987) were incorporated into the SEAPSO data set. Areal coverage by Sea Beam data varies from 35% in shallow water areas to 100% in deepwater areas. IFREMER used Regina software to reprocess these Sea Beam data after the cruises and to produce a smoothed and interpolated Sea Beam bathymetric map (Figure 3).

During the SEAPSO cruise, single-channel seismic data were collected using two water guns that had a total volume of 2.8 L and were fired every 10 s. After the cruise, some seismic sections were processed to convert time to depth, using regional velocity relationships that were obtained from interval velocities measured from seismic refraction experiments [*Pontoise and Tiffin*, 1986] and from multichannel seismic reflection data.

Magnetic data were collected using a proton-precession magnetometer. Residual magnetic anomalies were calculated using the 1980 International Geomagnetic Reference Field (IGRF 1980) updated to 1985. A Bodensee KSS30 gravity meter measured the gravity field; Eotvos corrections were made in real time, and then gravity data were reduced to free-air anomalies after corrections were calculated from the 1971 International Gravity Standardization Network (IGSN). All these data were reprocessed at IFREMER after final navigation was obtained.

SHALLOW STRUCTURE OF THE COLLISION ZONE

Subduction of aseismic ridges may produce complex tectonic patterns and sedimentary and erosional features in forearc rocks, depending on the size, orientation, and physical properties of both the ridge and the arc margin. In the NDR- New Hebrides collision zone, because of the small obliquity of the ridge relative to the direction of plate motion, the ridge moves northward along the arc, requiring a continual adjustment of the accretionary complex. This adjustment occurs in a complex three-dimensional environment and involves shortening due to normal trench convergence as well as lateral deformation related to the along-trench motion of the NDR. Conceptually, the lateral deformation occurs in three stages which we call shortening, uplift, and collapse (Figure 4). North of the ridge, this adjustment involves primarily shortening along thrust faults. Over the subducted part of the ridge, further adjustment of slope rocks involves mainly uplift and local collapse by slumping. South of the ridge, slope rocks collapse when they lose support as the ridge moves northward. This conceptual model, together with Sea Beam and single-channel seismic data, indicates that the collision zone consists of distinct northern, central and southern parts (Figure 5). In the next sections, we will first summarize the main geologic structures of the downgoing plate, and then we will describe, from north to south, the morphology and rock structure of the three parts of the collision zone.

Geology of the Oceanic Plate

On the oceanic plate, the NDR is a high-standing (2-4 km) feature that is 40 km wide and separates the deep West Santo Basin (WSB) from the Central d'Entrecasteaux Basin (CDB) (Figures 3 and 6).

The North d'Entrecasteaux ridge (NDR). The north flank of the NDR consists of gentle lower and steep upper slopes. The ridge crest decreases in relief and width close to the tectonic

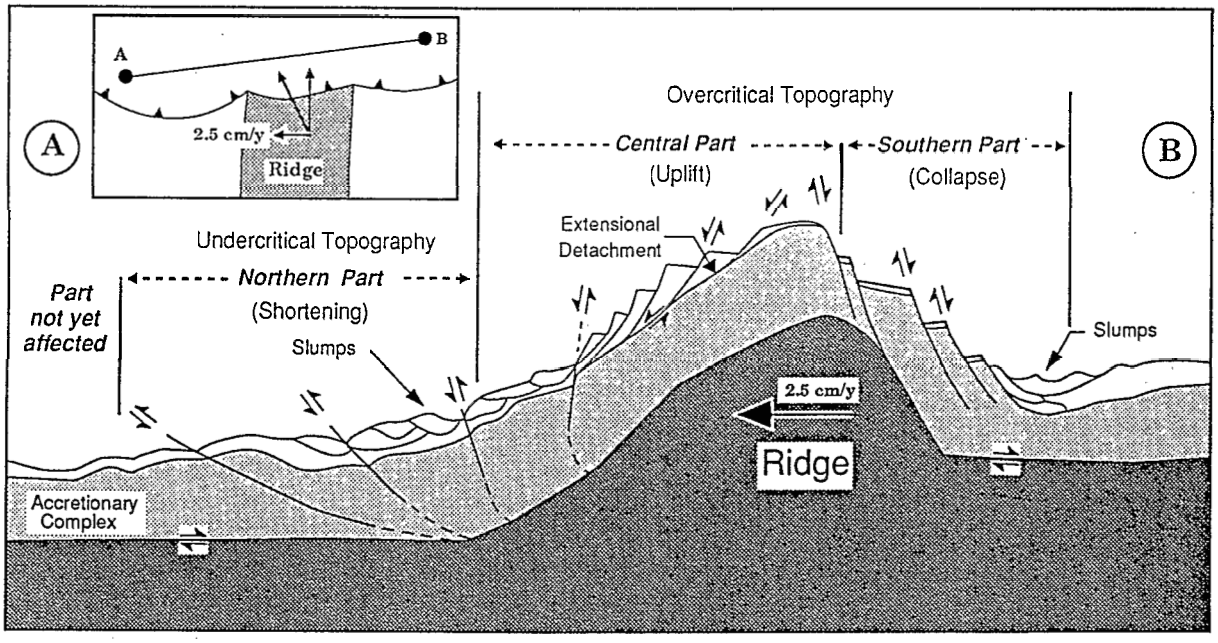

Fig. 4. Conceptual model of an accretionary complex in a collision zone between a ridge subducting obliquely and an island arc. The inset shows that this section is parallel to the trench, over the subducted part of the ridge. The section shows that the accreted rocks accommodate the lateral component of the ridge subduction by passing progressively through three stages of deformation identified from left to right as shortening, uplift, and collapse. The northern, central and southern parts of the collision zone are shown. In this conceptual model, the northern part is dominated by thrust and reverse faulting, and both the central and southern parts are structured by normal faulting and slumps.

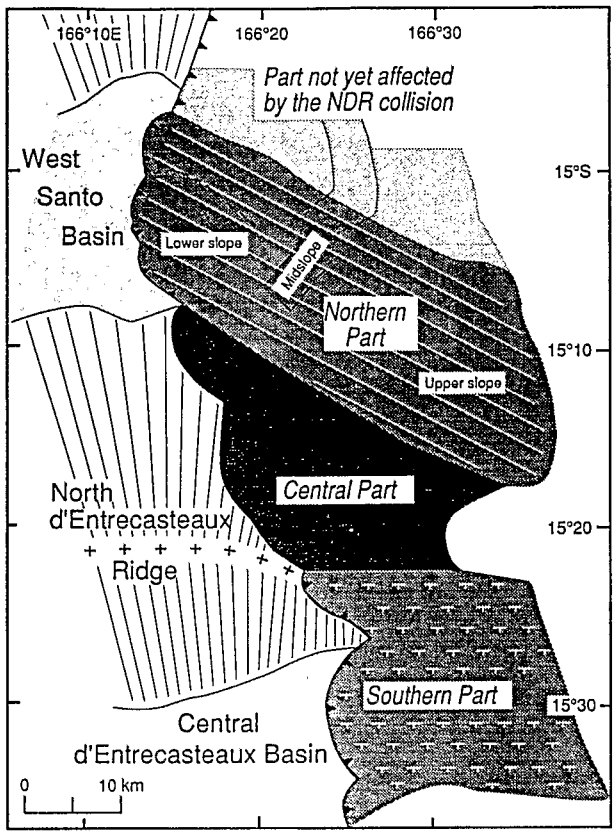

Fig. 5. The northern, central, and southern parts of the collision zone between the NDR and the New Hebrides island arc based on their morphologic and structural characteristics.

front and includes locally flat shoulders under water 3100 m deep. The south flank is locally steep (Figures 3 and 7). Numerous slumps cluster along the toe of the northern flank of the NDR, as suggested by the many flat topped seafloor bumps that are 100-300 m high and 3 km wide and are convex downslope (Figure 3). Support for this interpretation comes from seismic line 1113 (Figure 8, top), which shows that rocks from below the bumps return short reflections that occur above a continuous horizon.

Geologic and geophysical data show the structure of the NDR. A seismic refraction experiment indicates that the NDR has a high-velocity basement (5.95-6.0 km/s) that is overlain by about 2 km of rocks with velocity of 4.0 km/s [*Pontoise and Tiffin*, 1986]. Rocks were dredged from the basement and overlaying blanket of the ridge west of longitude 166°E. These dredge hauls recovered tuff and mid-oceanic ridge basalt (MORB) of early Eocene age [*Maillet et al.*, 1983]. Single-channel (Figure 7) and multichannel seismic reflection data [*Fisher et al.*, this issue] show that rocks forming the ridge return numerous discontinuous reflections, indicating that the upper part of the ridge includes layered rocks.

The magnetic anomaly map (Figure 9, top) shows that an east trending magnetic low, 180 nT in amplitude, is associated with the ridge and extends arcward across the accretionary complex. These magnetic data probably reveal the eastward extension of the NDR beneath the accretionary complex.

A simple magnetic model oriented north-south across the NDR was calculated using a two-dimensional modeling program [*Saltus and Blakely*, 1983]. This model indicates a magnetic body that thickens and extends from the WSB to below the northern shoulder of the NDR (Figure 9, bottom). Because no magnetic susceptibility are available from the NDR, we

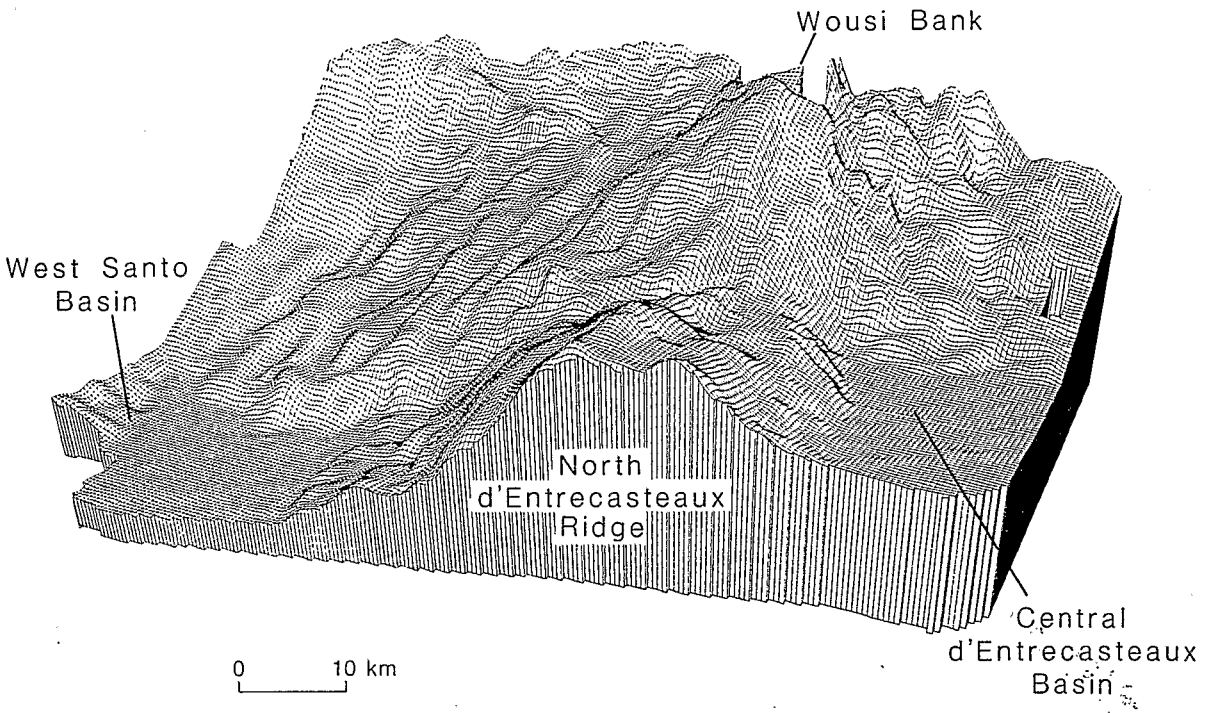

Fig. 6. Mesh diagram of the Sea Beam bathymetry of the collision zone between the NDR and the New Hebrides island arc. This diagram emphasizes the various morphologic patterns encountered from north to south along the arc slope: a smooth morphology in the part not yet affected by the NDR collision; a strongly oriented pattern in the northern part of the collision zone; a broad shallow protrusion (Wousi Bank) bounded by steep scarps in the central part of the collision zone; and a characteristic stepped-morphology in the southern part of the collision zone. Vertical exaggeration is 5:1.

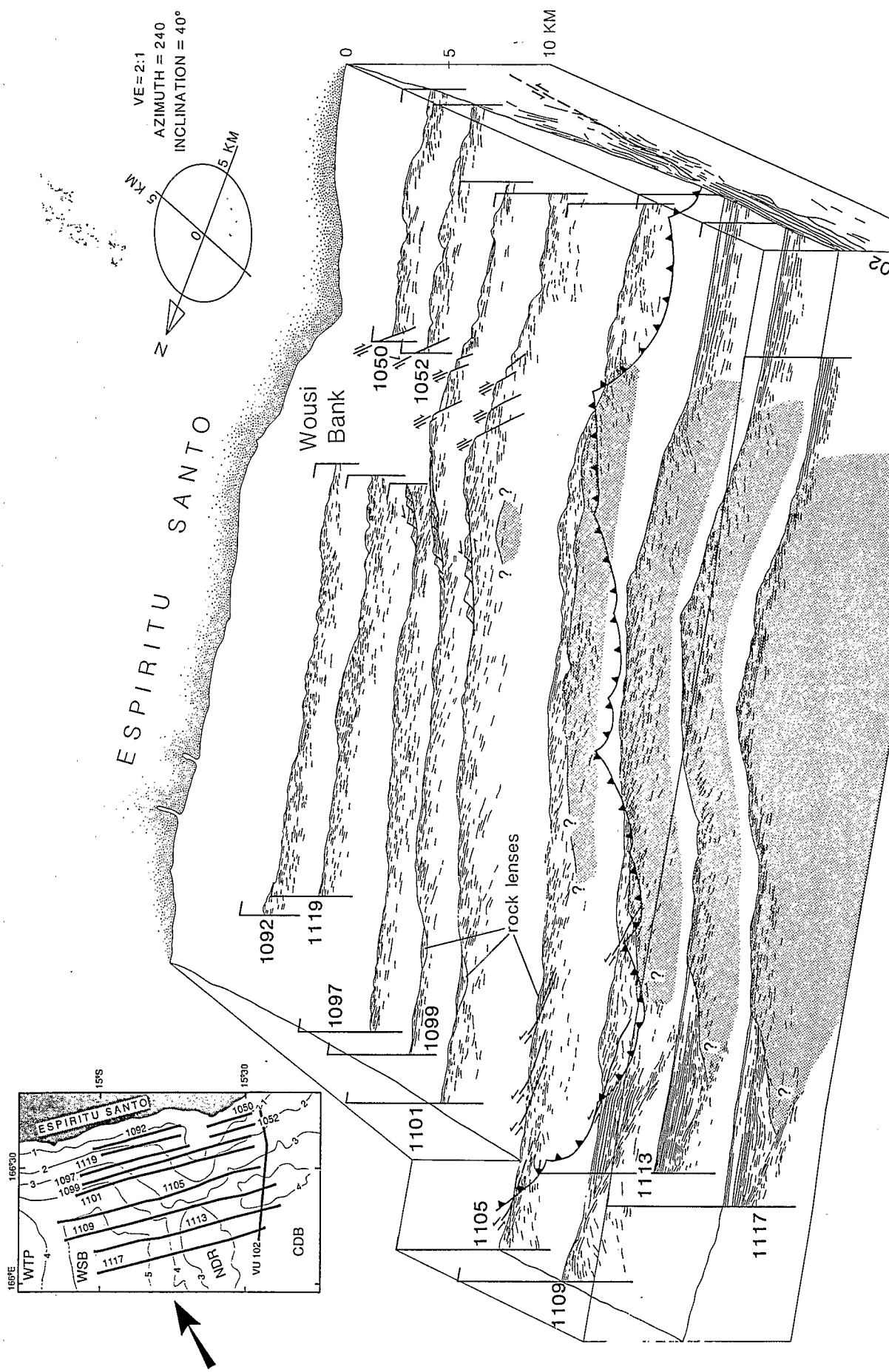
VE = 2:1
AZIMUTH = 240
INCLINATION = 40°
5 KM
5 KM
N
0
5
10 KM
ESPIRITU SANTO
Wousi Bank
1050
1052
1092
1119
1097
1099
1101
1105
1113
1109
1117
rock lenses
?
15°S
15°30
166°30
166°E
WTP
WSB
NDR
CDB
VU 102

used the lithology of dredged rocks and seismic refraction results to estimate the contrast in magnetic susceptibility between different magnetic bodies. From the recovered basalt [*Maillet et al.*, 1983] and the interpreted oceanic crust of the WSB [*Pontoise and Tiffin*, 1986] we infer that magnetic bodies of the ridge are higher in magnetization by 0.001-0.0025 than are poorly magnetic rocks of its basement. The absence of data from which to determine the relative strengths of induced and remanant magnetization for rocks of the NDR led us to assume that magnetic anomalies result wholly from induced magnetization. The purpose of the magnetic model (Figure 9, bottom) is to present one possible structure that accounts for the observed, ridge-parallel magnetic low. On the basis of gravity modelling and the similar seismic refraction velocities (6.0 km/s) measured in the basement rocks of the NDR and the WSB, *Collot and Fisher* [1988] proposed that the NDR might overlie an extension to the south of the oceanic crust that floors the WSB. The magnetic model shown here is consistent with this hypothesis.

The West Santo Basin (WSB). The WSB has a generally flat, smooth sea bottom (Figure 3) although on the basis of seafloor morphology, fans evidently issue from the NE and SE corners of this basin (Plate 1). In east-west cross section, both the basement and the fill of the West Santo Basin dip eastward and are unconformably overlain by a maximum of 500 m of subhorizontal trench fill turbidites [*Burne et al.*,1988]. From north to south, seismic data (Figure 7) indicate that the West Santo Basin contains a maximum of 1.5 km of flat-lying rocks that lie on two seismically distinguishable types of basement (Figure 8, top). The northern basement returns strong south dipping reflections from as deep as 1.6 km beneath the seafloor. On the basis of refraction velocities (4.04-5.23 km/s [*Pontoise and Tiffin*, 1986]), rocks of this basement may be either basalt or highly indurated sedimentary rocks. The top of the southern basement of the basin slopes northward and bounds a wedge of rocks that overlies the deepest part of the northern basement (Figure 7).

The Central d'Entrecasteaux Basin (CDB). The sea bottom of the CDB slopes gently arcward and is flat along the trench. Seismic data show the structure of the CDB and indicate that it contains about 1.5 km of well-bedded deposits. Multichannel seismic reflection profile 102 of *Fisher et al.* [this issue] shows that both basement and sediment of the CDB dip eastward and are unconformably overlain by a maximum of 400 m of trench fill deposits. North trending single-channel seismic profile 1113 (Figure 8) across the CDB indicates a gently south dipping discordance that separates the young trench fill deposits from a wedge of rocks resting against the NDR.

Close to the tectonic front, a 60-m-high closed morphologic feature shown in the detailed Sea Beam map (Plate 2) may be evidence for a mud volcano. Seismic line 1107 which cuts across this high shows that horizontal reflections are interrupted below the presumed mud volcano whereas they are continuous below the slumps of the tectonic front that are visible near the south end of the section (Figure 10).

Geology of the Accretionary Wedge Within the Collision Zone

The Northern Part of the Collision Zone.. The north boundary of the collision zone lies along a discontinuity in sea bottom morphology (Figures 3 and 6). North of this boundary, Sea Beam bathymetric data show that the arc slope is smooth except for local areas of rough topography and a slope break near 3800 m (Figure 11). Below this break (3800-5400 m) the slope dips about 6°, whereas above the break (1800-3800 m) it dips between 10° and 13°.

North of the collision zone, the structure of the accretionary complex is shown on multichannel seismic line 1024 (Figure 11). This seismic section shows a band of high-amplitude reflections that correlates with the subducting oceanic strata. Although rocks that overlie the subducting strata are poorly reflective, a few discontinuous, faint reflections dip consistently trenchward. Some arcward dipping events that terminate downdip against the subducting oceanic strata are interpreted as thrust faults. These faults indicate that the interplate thrust fault lies along the oceanic strata.

The northern part of the collision zone exhibits a strong morphological grain that is characterized by lineaments that include numerous small-relief (50-200 m in height and 500-3000 m in width) ridges, canyons, and valleys that are consistently oriented obliquely (N60°W) to the slope and define an important morphologic trend. This grain is evident in the mesh diagram of Sea Beam data (Figure 6).

We recognize three slope areas that are bounded by major transverse breaks in slope. Sea Beam data indicate that the break in slope that lies north of the collision zone, near 3800 m, extends southward into the collision zone. This slope break together with a less well defined one located near 3000 m separate an undulating, gently dipping (4°-6°) lower slope, a more steeply dipping (8°-12°) midslope, and a irregularly dipping (4°-6°) upper slope (Figure 5).

The gently dipping lower slope is formed by three lobes that protrude toward the trench axis (Plate 1). The lobes consist of smooth ridges separated by low-relief valleys that do not parallel the overall N20°W strike of the arc, but instead the valleys trend obliquely (N40°W to N115°W) across the arc slope (Figure 12).

Some morphologic lineaments that trend obliquely (N60°W) across the arc slope can be traced trenchward along valleys to cusps in the tectonic front, where this front shows east-west relative offset (Figure 3). For example, the southern lobe (Plate 1) is sharply offset southeastward along a straight lineament by about 4 km with respect to the central lobe. This offset suggests that an apparent left-lateral strike-slip movement (Figure 12) occurred along the boundary between these lobes.

Fig. 7. Fence diagram showing the shallow structure of the NDR-New Hebrides collision zone from depth-converted seismic data. The grey shade indicates rocks of the North d'Entrecasteaux ridge as they enter the subduction zone. The barbed line indicates the trace of the interplate decollement. The inset in the upper left corner shows the location of seismic lines used in the diagram and the azimuth of view (N240° W). Heavy numbers refer to SEAPSO single-channel seismic lines and VU 102 is a U.S. Geological Survey multichannel seismic line. This line was projected onto the southern edge of the diagram.

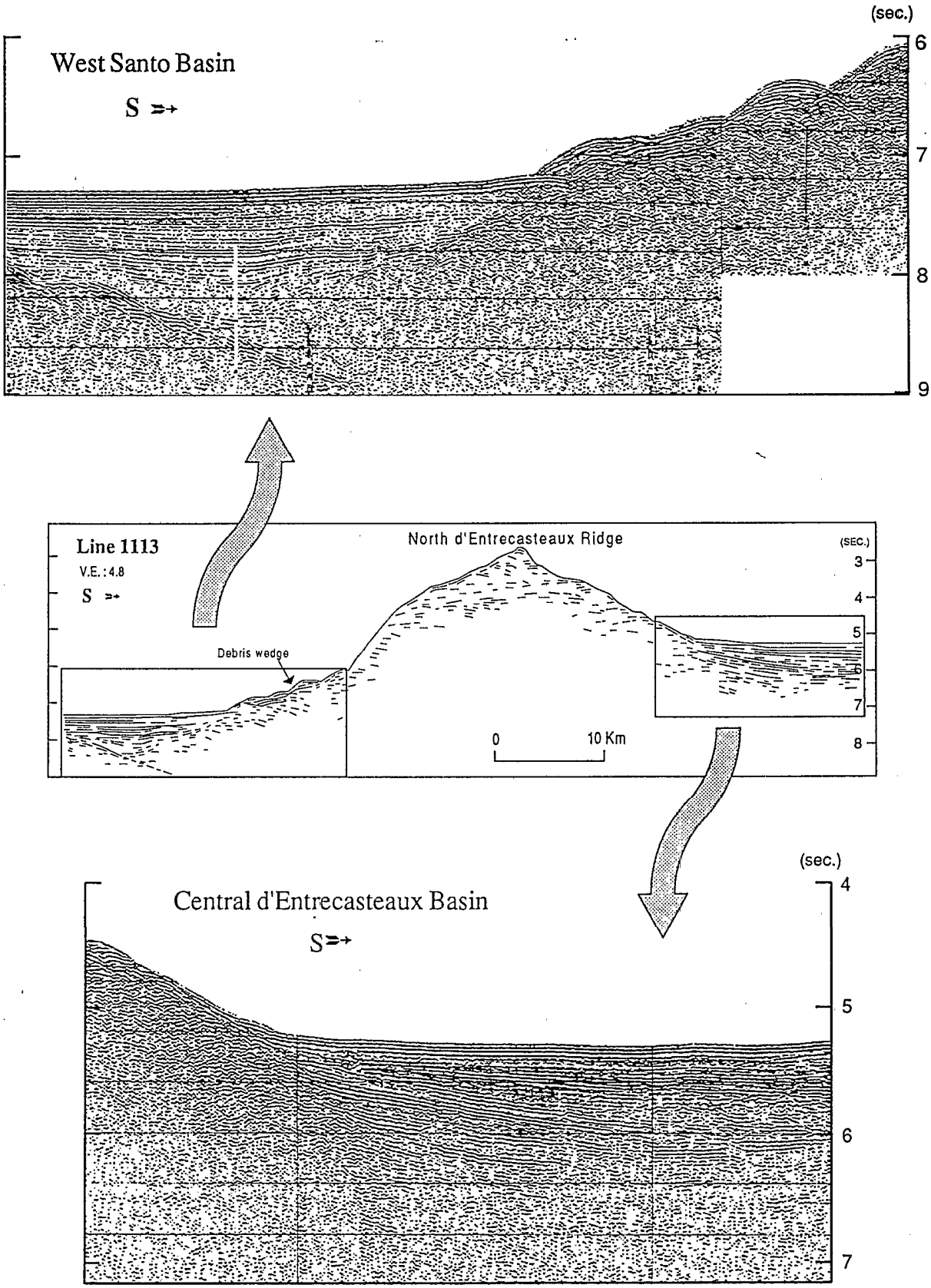

Fig. 8. Single-channel seismic data and line drawing for section 1113 across the North d'Entrecasteaux Ridge and adjacent West Santo and Central d'Entrecasteaux basins. Location is shown in Figure 3.

Plate 3. Detailed Sea Beam bathymetric map showing the fine-grained structure of the upper slope in the northern and central parts of the collision zone. A drainage network is formed by a major arcuate canyon and numerous east trending canyons. The N60ºW trending steep scarp north of the Wousi Bank separates the northern and central parts of the collision zone. Bathymetric contour interval is 20 m. Location of this area is shown in Figure 3.

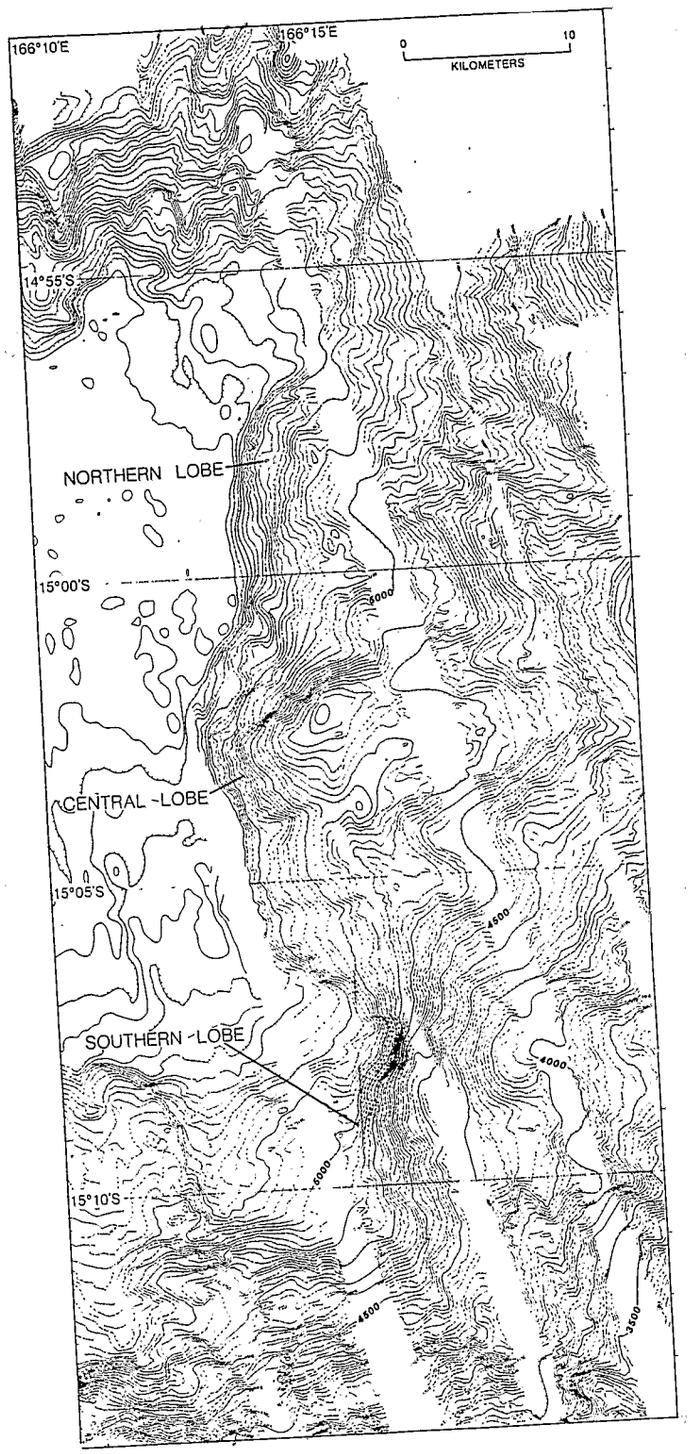

Plate 1. Detailed Sea Beam bathymetry showing the lobate structure of the lower accretionary complex in the northern part of the collision zone. Bathymetric contour interval is 20 m. Location of this area is shown in Figure 3.

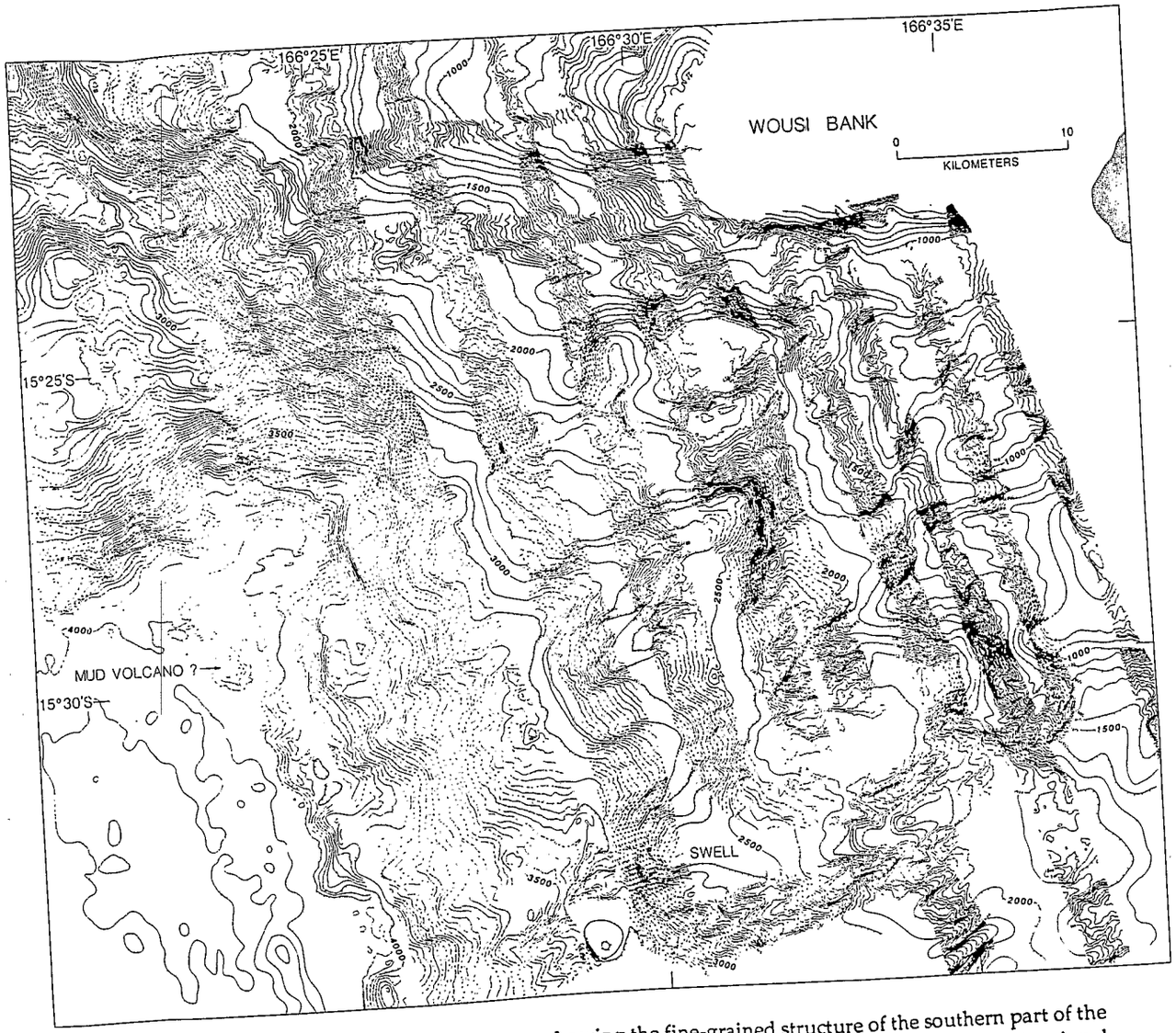

Plate 2. Detailed Sea Beam bathymetric map showing the fine-grained structure of the southern part of the collision zone. Steep scarps, flat hanging wall terraces, and large lobate bodies suggest that extensional tectonics and mass wasting dominate the structural development of this part of the accretionary complex. The highly irregular morphology of the lowermost slope suggests that the deformation front is masked by slumped rocks. Location is shown in Figure 3.

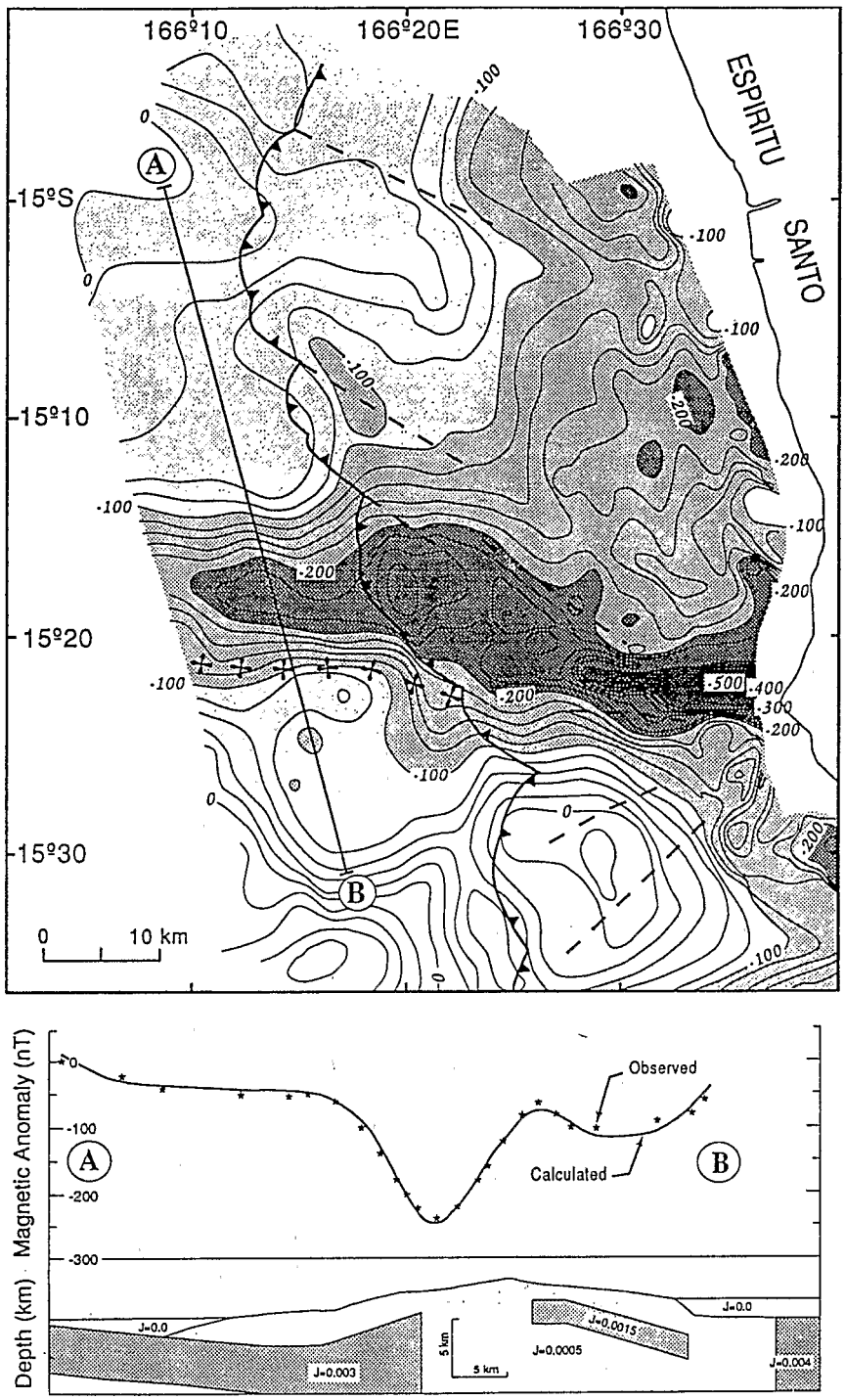

Fig. 9. (Top) magnetic anomalies over the collision zone between the NDR and the New Hebrides island arc. Magnetic contour interval is 20 nT. The negative magnetic anomaly associated with the ridge extends landward beneath the accretionary complex. Barbed line shows the trace of the interplate decollement, and dashed lines show the major faults. Crosses show the ridge crest location. (Bottom) Two-dimension magnetic model across the NDR; a constant 70-nT regional value was removed from the calculated anomaly to match the average level of the observed magnetic data; J is magnetization in gauss.

Although lineaments are evident primarily in morphologic data, single-channel seismic reflection profiles show that some of them lie along the surface traces of thrust faults that crosscut the accretionary wedge. Seismic profile 1107 (Figure 13) shows that strata within the lower accretionary complex return flat or curved, discontinuous events that can be interpreted as disrupted and folded rock layers. These deformed layers are locally interrupted by reflectors with an apparent south dip. We interpret these dipping reflectors as thrust faults, some of which can be traced upward to the lineaments that we describe

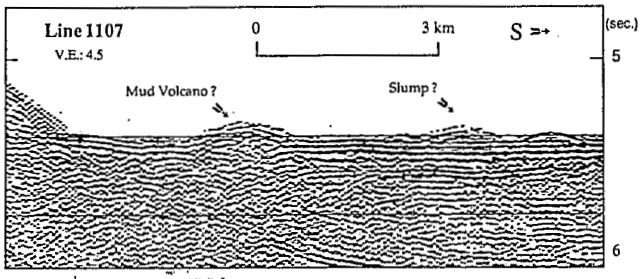

Fig. 10. Part of single-channel line 1107 across the Central d'Entrecasteaux Basin showing a possible mud volcano also depicted as a 60 m closed high in Figure 15. Location is shown in Figure 3.

above (Figure 12). Close to the tectonic front, the surface trace of some thrust faults appears to be parallel to the trench. Crossing seismic lines suggest that in the lower accretionary complex, most of the thrust faults dip south to southeast, but some of them dip east. Several steep, south dipping reverse faults are clearly imaged in migrated multichannel seismic reflection line 106 [*Fisher et al.*, this issue] (Figure 12). These reverse faults closely coincide in location with the N60°W trending strike-slip lineament between the central and southern lobes.

In addition to faults and folds, the lower slope is deformed by mass wasting. Across the lower slope, Sea Beam data indicate lobate bodies that are 0.5-5 km wide and elongate downslope. Single-channel seismic reflection section 1103

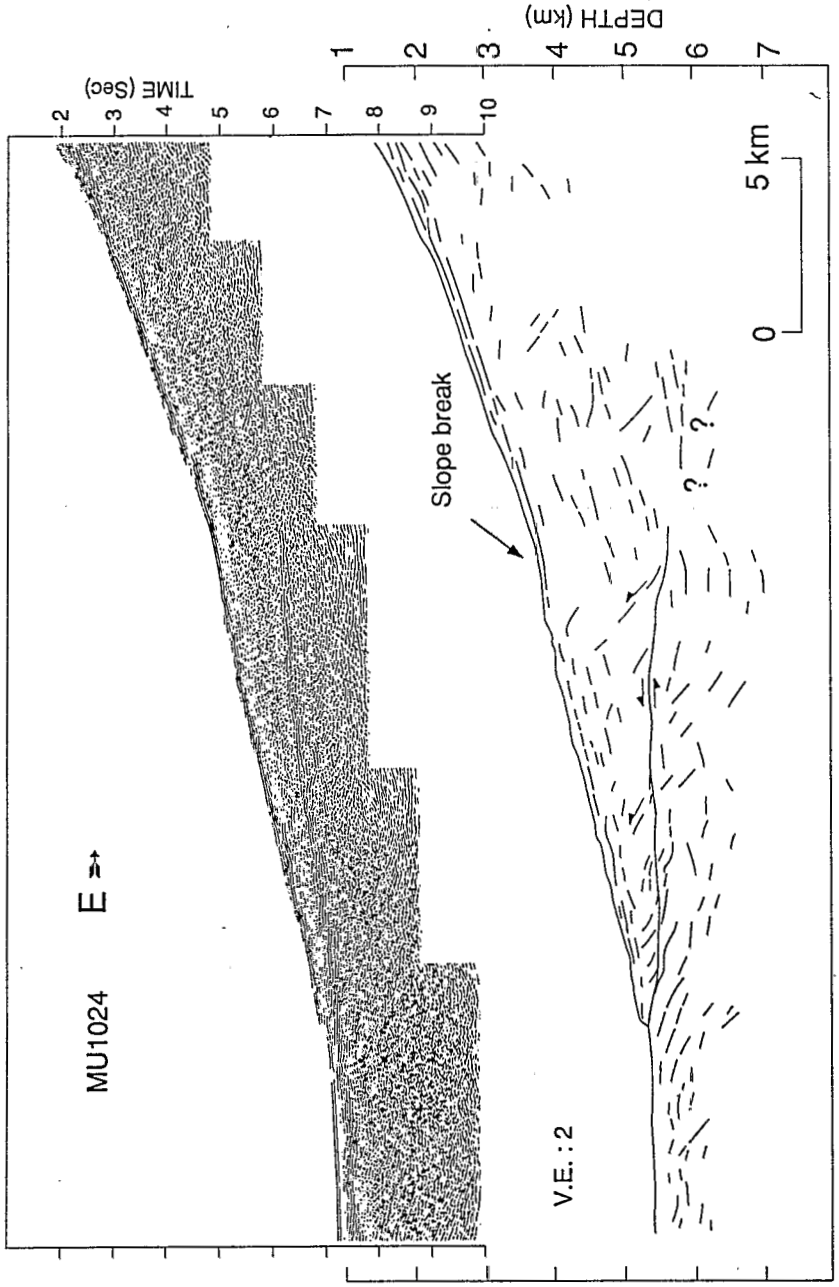

Fig. 11. Multichannel seismic section MULTIPSO 1024 and corresponding depth converted section showing the structure of the accretionary complex north of the collision zone. Location is shown in Figure 3.

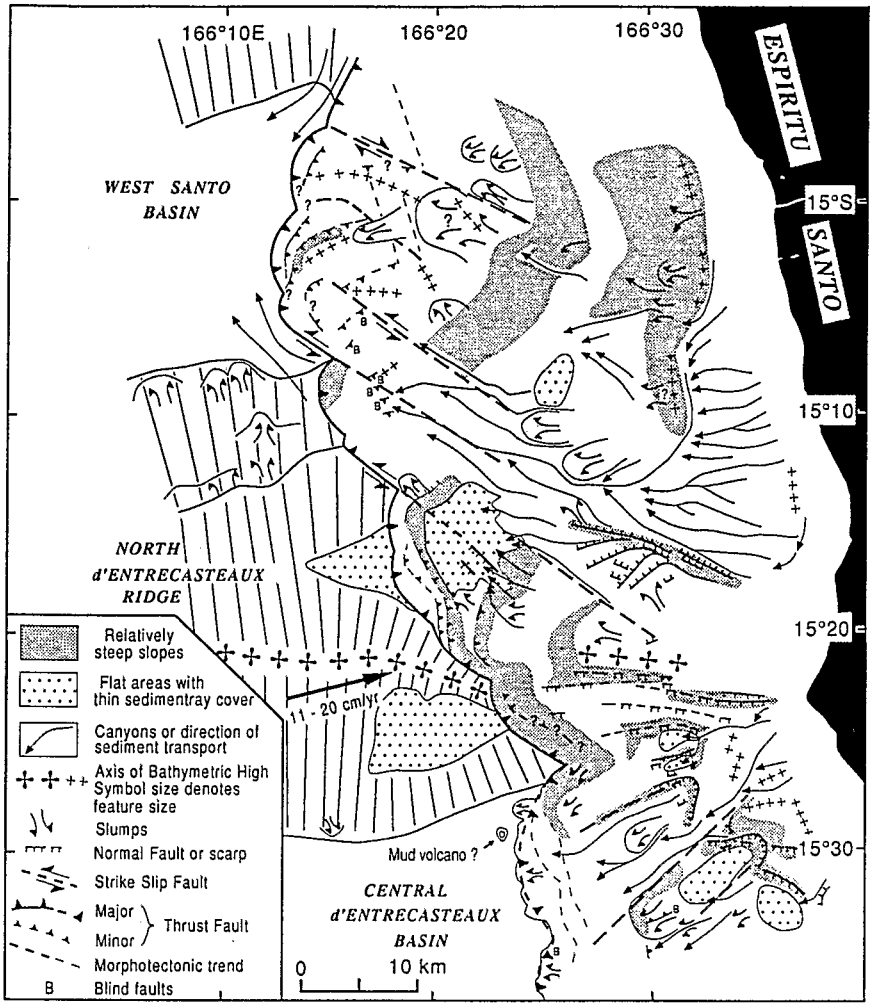

Fig. 12. Tectonic interpretation of the collision zone between the NDR and the New Hebrides island arc, based on morphologic and seismic reflection data.

(Figure 14), which cuts perpendicularly through one of these bodies, shows what appears to be a lens of rock that returns faint, disorganized reflections. A few reflections can be traced below the rock lens suggesting either an unconformity or a detachment surface. Other seismic lines, 1105, 1101 and 1099 (Figure 7) also indicate the presence of rock lenses. Hence slumps or debris flows may form at least the shallow part of the lower accretionary complex (Figure 12).

In contrast to the gentle dip of the lower slope, the steeper midslope of the northern part of the collision zone bulges seaward and diverges by 45° eastward from the regional arc trend. This divergence indicates that the midslope was apparently rotated clockwise by about 45° relative to its trend (N20°W) north of the collision zone (Figure 12). Such a rotation would involve left-lateral displacement between the northern and central parts of the collision zone. This sense of displacement is consistent with the apparent left-lateral offset along the suggested N60°W trending strike-slip fault that separates the central and southern lobes. Alternatively, the 45° divergence of the midslope from the regional arc trend could result from a local northward tilt of the accretionary complex.

The morphology of the upper slope above 2000 m (Plate 3) includes numerous deeply incised, submarine canyons and intervening sharp ridges that define a drainage network. This network converges to a major, arcuate canyon that follows the widespread N60°W tectonic trend and forms the most integrated sediment system that feeds the arc slope of the northern part of the collision zone (Figure 12).

West of a small ridge (Plate 3), the upper slope exhibits small flat areas, numerous small lobate bodies, and elongated highs that are 50-100 m in amplitude and small canyons. Multichannel seismic section 105 (Figure 15) shows the structure of the rocks beneath this upper slope. This section indicates that at least half of the thickness of the accretionary complex consists of rocks returning short overlapping reflections that dip and shift consistently northwestward [*Fisher et al.*, this issue]. Such a structure strongly suggests that slump debris accumulated to form a large part of the accretionary complex below the upper slope.

The central part of the collision zone: A strongly uplifted area. The major feature of slope morphology in the central part of the collision zone is the broad protrusion that cuts transversely across the slope and culminates in the Wousi Bank, which reaches almost to sea level (Figures 3 and 6). This protrusion is bounded on both north and south by relatively steep scarps that are as high as 500-800 m and dip 30°-40°. The scarp that

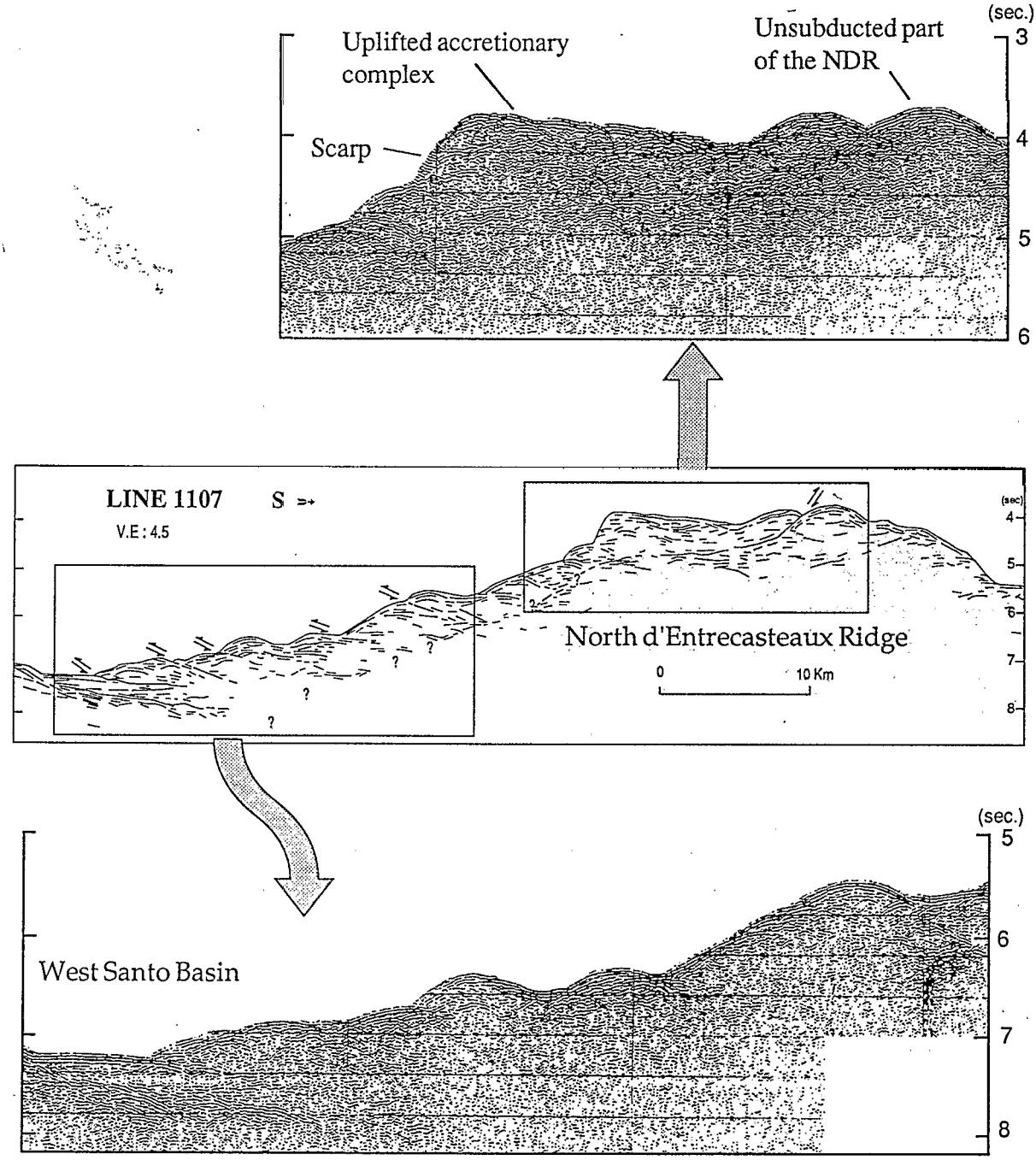

Fig.13. Single-channel seismic data and line drawing for section 1107 that cuts across the lower accretionary complex parallel to the trench. Location is shown in Figure 3. (Top) Enlargement of the seismic data revealing the flat shoulder of the ridge beneath the accretionary complex; (Bottom) part of the seismic section showing thrust faults and small folds that form the lobes of the wedge toe.

separates the northern and central parts of the collision zone trends N60°W and appears to extend along a major tectonic lineament to a cusp in the tectonic front that indicates left-lateral offset (Figure 12). This linear extension indicates that the scarp may have a tectonic origin rather than an erosional origin. The zone of scarps that separates the central and southern parts of the collision zone trends west, parallel to the NDR and connects westward to a minor cusp in the deformation front.

The tectonic front of the central part of the collision zone has a lobate morphology that shows a few sinuous trench-parallel lineaments and two remarkable scarps. One scarp forms the western side of the southern lobe (Plate 1), and the other one forms the northern edge of a flat terrace located near 2750 m (15°14'S, 166°20'E in Figure 3). These two scarps dip 25°-30° and have reliefs of between 400 and 600 m. They lie above cusps of the tectonic front that suggest left-lateral offset (Figure 12). Both the scarps and the offsets of the tectonic front

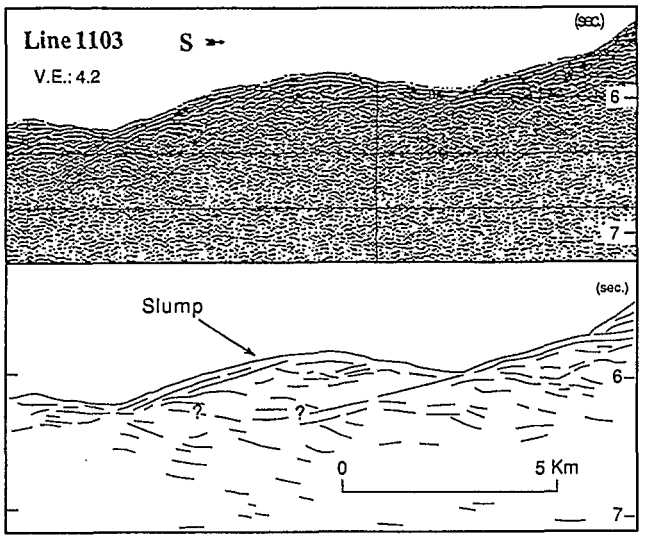

Fig. 14. Part of single-channel line 1103 across the lower accretionary complex in the northern part of the collision zone showing a possible slump. Location is shown in Figure 3.

coincide in location with major breaks in slope at the toe and midslope of the north flank of the NDR. The coincidence between frontal scarps and lateral offsets of the tectonic front and breaks in the slope of the NDR indicates that the ridge shape controls the formation of these scarps as well as the development of the suggested left-lateral strike-slip faults that transect the accretionary complex.

Single-channel seismic line 1107 (Figure 13, top) shows the structure of the lower accretionary complex above the subducted part of the ridge. On this north-south cross section, a band of high-amplitude reflections extends northward from the unsubducted part of the ridge and indicates the top of the NDR beneath the accretionary complex. Reflections from within the accretionary complex above the ridge are discontinuous but no thrust faults within this part of the accretionary complex are evident from our data (Figure 13, top). However, multichannel seismic data suggest that the high-amplitude reflections from the top of the ridge is the decollement [*Fisher et al.*, this issue].

Beneath the upper slope of the central part of the collision zone, Sea Beam and seismic data show that local collapse occurs along a detachment surface. Sea Beam data indicate that the northwest slope of the Wousi Bank is stepped along small, flat terraces separated by short scarps that trend from N60°W to N120°W (Plate3 and Figure 14). Sea Beam data also show that these scarps are gouged by numerous small canyons that trend northwest. Single-channel seismic section 1123 (Figure 16) shows the structure of the central part of the collision zone. Although diffraction tails generated by the rough seafloor complicate the seismic image, line 1123 shows an almost continuous north-dipping reflection that lies about 300 m below the seabottom. Short subhorizontal events returned by the shallow rocks are offset by normal faults that terminate downdip against the major north dipping reflection. From these data, we interpret the north dipping horizon as an extensional detachment surface along which overlaying sediment failed by slumping. Other single-channel seismic sections (Figure 7) support this idea of local collapse, which indicates a highly unstable northwest flank of the Wousi Bank.

The Southern Part of the Collision Zone: An Area of Collapse. In the southern part of the collision zone, the upper slope of the arc exhibits an uneven morphology that contrasts with the lower slope, below 3000 m, which has a smooth morphology but an irregular tectonic front (Plate 2).

The upper arc slope that forms the south flank of the Wousi Bank is offset vertically by major scarps as high as 800 m that trend west, parallel to the NDR. These scarps locally bound flat terraces. Single-channel seismic reflection profile 1125 (Figure 17) shows that a thin, nearly horizontal sediment layer covers the terraces. Rocks below this layer return groups of faint, discontinuous reflections, indicating that strata beneath the arc slope are disrupted. Although fault planes are not clearly imaged in our single-channel seismic data, the morphology of the scarps and their location in the wake of the NDR suggest that the thin sedimentary blanket covers blocks that are downdropped along normal faults (Figure 17, bottom).

The upper arc slope is also marked by morphologic lineaments that are oblique (N45°E-N60°E) to the arc slope (Figure12) and do not show clear evidence for strike-slip motion. However, these lineaments appear in plan view to be conjugate to the N60°W trending lineaments of the possible strike-slip faults evident in the northern part of the collision zone.

Other irregularities of the upper arc slope include a canyon network that parallels the N60°E trending lineament as well as seafloor swells that bulge westward. The most prominent swell is located at 166°30'E, 15°33'S in Plate 2 and is 400-600 m high and 4 km wide. This swell can be correlated in position with steep-sided topographic reentrants located just upslope. We suggest that this swell is a slump and the corresponding upslope reentrant is a slump scar.

In contrast to the irregular topography of the upper slope, the lower slope shows some trench-parallel lineaments but is relatively smooth. However, the tectonic front exhibits small-scale irregularities as well as a narrow band of closed morphologic highs and lows that may indicate slump debris. In addition to this irregular morphology, the seismic image of the tectonic front, as indicated by multichannel seismic reflection profile 102 of *Fisher et al.*, [this issue], reveals that the tectonic front may be buried beneath slumps.

DEFORMATION AND TECTONIC EROSION OF ARC SLOPE ROCKS IN THE COLLISION ZONE

The morphology of the accretionary complex provides qualitative information about the overall deformation of the accretionary complex. In this section, we discuss the mechanics of deformation of the accretionary complex that results from the collision between the NDR and the New Hebrides island arc.

Sea Beam and seismic reflection data collected over the three parts of this collision zone show evidence for shortening, uplift, and collapse, the three stages of deformation that are introduced in a conceptual model (Figure 4). However, the mechanics of deformation of the accretionary complex is greatly complicated by the three-dimensional aspect of the collision zone. For example, the simplified model (Figure 4) accounts for neither trench-parallel structures nor for extrusion of arc slope rocks toward the trench.

In the following parts of this section we discuss the occurrence of trench-parallel structures; the thickening of the accretionary complex along thrust faults that trend mainly

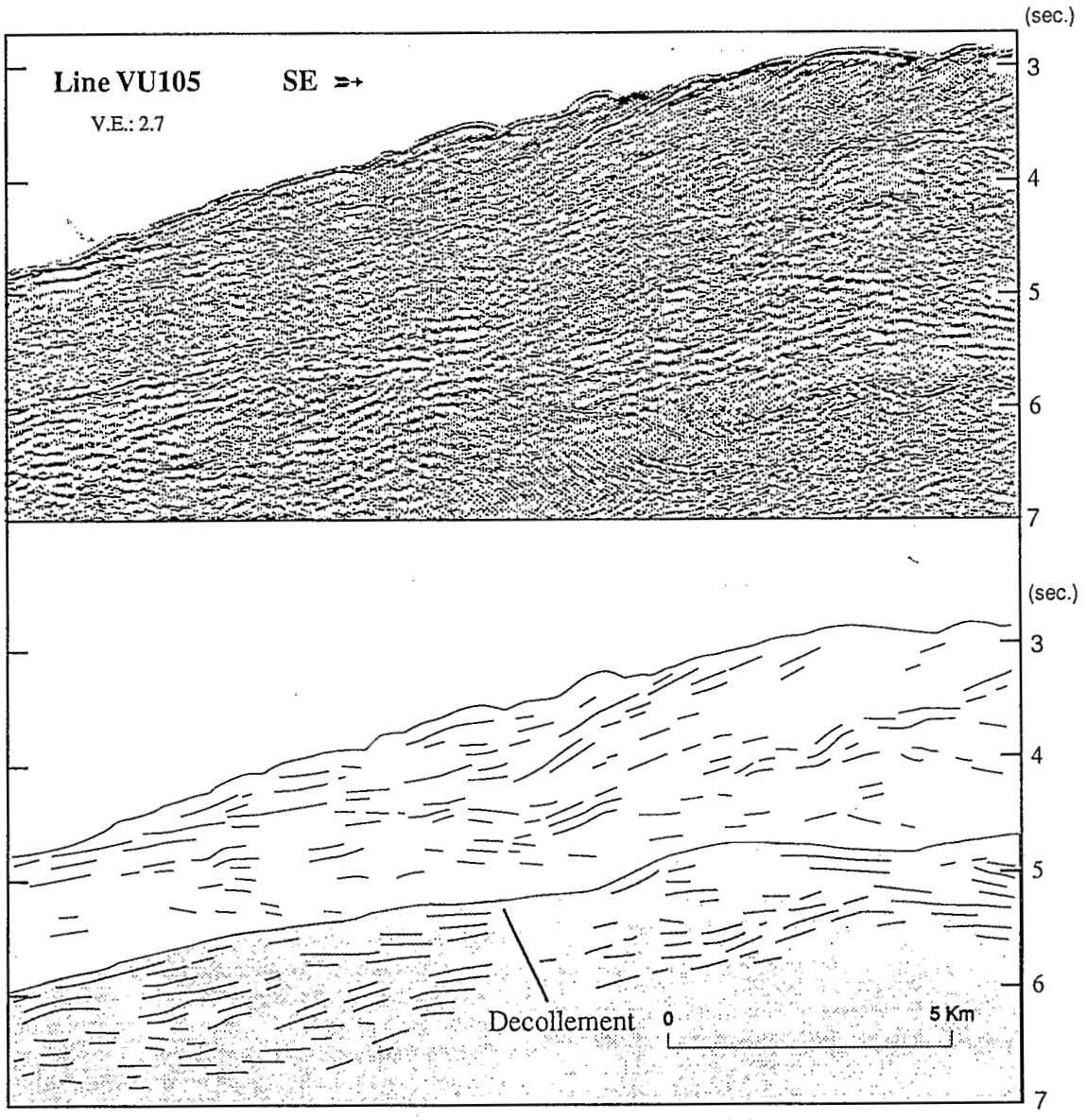

Fig. 15. Migrated and interpreted sections for multichannel seismic line VU105. Shaded area indicates the subducting northern flank of the NDR. Overlapping horizons with seaward dips suggest that slumps constitute at least 50% of the thickness of the accretionary complex. Location is shown in Figure 3.

oblique to the arc slope; the extrusion, uplift, and tectonic erosion of arc slope rocks; and the extent of the area involved in the collision zone.

Trench-Parallel Structures

Trench-parallel structures classically develop in accretionary wedges along convergent margins. In the NDR-New Hebrides arc collision zone, trench-parallel structures should be well developed in the lower accretionary complex because normal trench convergence is faster than along-trench motion of the NDR. Sea Beam morphology and seismic data, however, suggest that trench-parallel structures are poorly developed in all three parts of the collision zone. A few morphologic lineaments parallel the tectonic front near the toe of the accretionary complex (Figure 12). These lineaments may either mark downslope boundaries of slump masses or the surface traces of thrust faults. Multichannel seismic reflection line 104 [*Fisher et al.*, 1986] cuts trough the arc slope in the central part of the collision zone and does not show clear evidence for thrust faults in the accreted rocks. These faults may not be imaged clearly on seismic section 104 because strain due to collision may not concentrate along thrust fault planes but instead may penetrate throughout the fractured arc slope rocks. Therefore, the apparently poor development of trench-parallel structures may be related to the processes of collision.

Indentation and Thickening

Lallemand and Le Pichon [1987] used the concept of the critical taper of accretionary wedges [*Davis et al.*, 1983] to propose that when a seamount begins to subduct, the dip of the decollement increases adjacent to the trench so that in most cases the arc slope becomes undercritical and shortens. Shortening and

slope failure lead to formation of an indentation in the lower arc slope and thickening of the wedge along thrust faults.

Slope indentations in forearc areas are commonly reported from Sea Beam data collected in collision zones [*Daniel et al.* 1986; *Pontoise et al.*, 1986; *Kobayashi et al.*, 1987; *Le Pichon et al.*, 1987; *Collot and Fisher*, 1989], and thickening of the accretionary wedge along thrust faults was reported from the collision zone of the Daiichi Kashima seamount with the lower slope off Japan [*Lallemand et al.*, 1989]. In contrast to the above observations, no indentation in the arc slope is evident landward of the NDR, and as mentioned earlier in this report, multichannel seismic reflection data do not show clear evidence for east dipping thrust faults in the accreted rocks of the central part of the collision zone. The absence of an indentation suggests that the ridge has already passed the early stage of collision described by *Lallemand and Le Pichon*, [1987].

Thickening of the accretionary complex is more readily evident in the northern part of the collision zone than in the central part. In this northern part, the south to southeast dipping thrust and steep reverse faults indicate that the lower accretionary complex shortens in a N-S direction. Inasmuch as the NDR slowly creeps northward beneath the accretionary complex, the dip of the decollement must increase from nearly flat above the subducted West Santo Basin to 13° above the north flank of the ridge (Figure 4). Consequently, because of

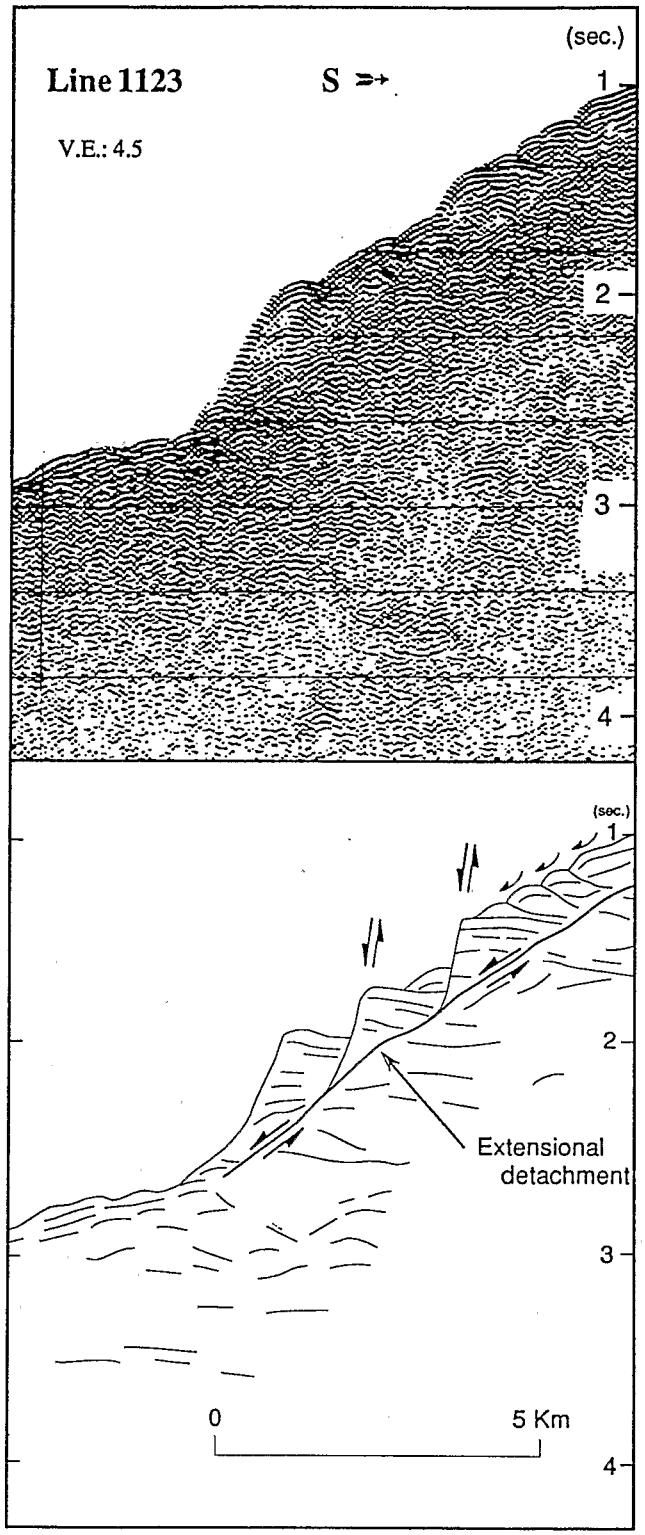

Fig. 16. Single-channel seismic section 1123 and corresponding line drawing across the northern flank of the Wousi Bank. This section shows slump blocks bounded by normal faults that merge along an extensional detachment. Location is shown in Figure 3.

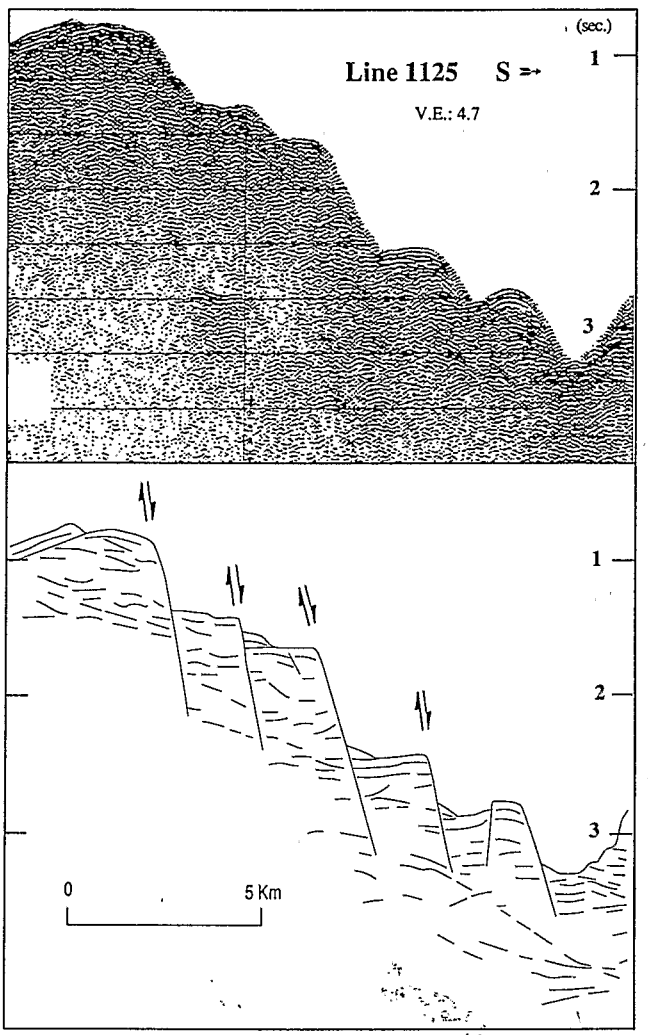

Fig. 17. Single-channel seismic section 1125 and corresponding line drawing across the southern part of the collision zone. This section shows possible normal faults generated by the collapse of the accretionary complex after the ridge passage. Location is shown in Figure 3.

the oversteepening of the base of the wedge [*Lallemand and Le Pichon*, 1987], the lower accretionary complex of the northern part of the collision zone becomes undercritical and must grow by internal thrusting to maintain a critical taper.

Lateral Extrusion of Arc Slope Rocks.

As the ridge starts to collide, lateral extrusion of arc slope rocks results from impingement of the NDR against the arc slope. This type of lateral deformation has been described for large-scale continental collision by *Tapponnier and Molnar* [1976]. In one conceptual model of an arc-ridge collision zone, the extrusion reduces the amount of uplift and takes place along curvilinear strike-slip faults that are oblique to the arc slope and cause slope rocks to bulge toward the trench on both sides of the ridge [*Collot et al.*, 1985]. In the collision zone between the NDR and the New Hebrides island arc, the conjugate structural pattern, defined by tectonic lineaments that trend N53° to N60°W in the northern part of the collision zone and by other lineaments trending N46°E to N60°E in the southern part (Figure 12), may have resulted from impingement of the ridge against the arc. Seaward bulges of accreted rocks such as the lobes in the northern part of the collision zone could also have resulted from lateral deformation caused by ridge impingement against the arc. However, both the lobes and the N60°W trending lineaments are more readily evident in the northern part of the collision zone than they are in the southern part, where large east trending normal faults predominate. This structural contrast suggests that lateral deformation of the accretionary complex is mainly accomplished by the northward component of the ridge motion.

Detailed bathymetric data can be interpreted in agreement with seismological studies [*Isacks et al.*, 1981] that the northward component of the ridge motion is small (2.5 cm/yr). In the corner formed by the north flank of the ridge and the tectonic front, accreted rocks are displaced arcward along the suggested N60°W trending fault that separates the northern and central parts of the collision zone. If the ridge subducts nearly parallel to the trench, the accretionary complex would have been extruded seaward along the north flank of the ridge and filled this corner. The absence of such corner fill as well as the suggested displacement of accreted material along the N60°W trending strike-slip fault are consistent with the inference of a small obliquity to the arc-ridge convergence.

Accreted rocks near the north flank of the ridge are deformed by transpression, and trenchward extrusion occurs farther north in the northern part of the collision zone. The concept of rock extrusion is supported by the protrusion of the lobes across the trench along N60°W trending strike-slip faults. However, the motion along the strike-slip fault that separates the central and southern lobes may not be purely strike-slip but transpressive, as indicated by the close correspondence in location between south dipping reverse faults and the inferred left-lateral strike-slip fault (Figure 12). We believe that close to the north flank of the ridge, deformation of the accretionary complex is mainly accomplished through transpression.

Factors other than the obliquity of subduction of the NDR, such as mass wasting and variation of shear stress along the decollement, may affect the deformation and displacement of arc slope rocks in the northern part of the collision zone. Numerous topographic features across the lower accretionary wedge attest to mass wasting. We believe that slumps are triggered from the midslope that is oversteepened by the northward creeping ridge, which makes room for itself beneath the accretionary complex. These slumps come to rest on the lower arc slope and contribute to the growth and the protrusion of the lobes across the trench.

The horizontal offset between the central and southern lobes may reflect a change in the basal friction below these lobes. This offset correlates in location with the abrupt morphologic and lithologic change between the presumably water-rich turbidites of the West Santo Basin and the debris wedge of the lower slope of the NDR. We infer that this change in morphology and lithology of the subducting rocks decreases the basal friction beneath the central lobe relative to the friction below the southern lobe. This decrease facilitates seaward extrusion of arc rocks. Conversely, the inferred relative increase in basal friction below the southern lobe could facilitate transportation of accreted rocks arcward across the ridge.

Uplift, Tectonic Erosion, and Mass Wasting

Uplift and tectonic erosion of arc slope rocks occur in all three parts of the collision zone but predominate in the central and southern parts. In the northern part of the collision zone, uplift of the upper slope is inferred from rock stratification. Seismic line 105 (Figure 15) that trends across the upper slope shows several shallow rock bodies with divergent overlapping reflectors that dip consistently trenchward. This stratification suggests that slope material slid downslope, stabilized, and then was remobilized. Repeated mobilization of accreted rocks occurs as the NDR migrates northward and uplifts the accretionary complex.

In the central part of the collision zone, geophysical data reveal that the Wousi Bank has been greatly uplifted and that extensional tectonics predominates over compressive tectonics. The Wousi Bank is bounded on its northern and southern sides by steep scarps and normal faults whose cumulative separation indicates that rocks of the Wousi Bank have been uplifted by about 1500-2500 m relative to arc slope rocks in the northern part of the collision zone.

The sea bottom over the northwestern flank of the Wousi Bank slopes southward across a series of slump blocks that failed along an extensional detachment (Figure 16). This structure indicates that in the central part of the collision zone, the accretionary complex has an overcritical topography, as indicated in Figure 4. Therefore, we believe that rocks of the arc slope in the central part of the collision zone accommodate the ridge subduction mainly by uplift and by tectonic erosion that involves local collapse. This tectonic erosion helps to remove shallow weak rocks from the accretionary complex and hence may expose strong rocks from deeper levels in the wedge.

In the southern part of the collision zone, the structure of the arc slope is mostly controlled by gravity tectonics as shown by features interpreted to be large normal faults (Figure 17) and slumps. We believe that because large normal faults trend parallel to the NDR, the collapse of the arc slope is due to the loss of support as the NDR withdraws northward (Figure 4), and the volume once occupied by the ridge must be filled by arc slope rocks.

Large-scale mass wasting may have produced overpressures in the subducting sediment of the southern part of the collision zone. Abrupt loading of oceanic sediment of the CDB by slump masses could increase pore pressure within these sediments. This overpressure may account for a possible

mud volcano near the toe of the slope in the CDB (Figure 10).

Sea Beam and seismic reflection data indicate that in this collision zone, mass wasting debris rests on the arc slope and part of it is transported to the trench where it is subducted. The approximate volume of accreted rocks displaced by the subducting ridge is about 2300 km^3. Part of these displaced rocks reside as slumps on the arc slope, as indicated by multichannel seismic lines 102 and 105 [*Fisher et al., this issue*]. However, some of the displaced rocks are transported to the trench as indicated by canyons on the arc slope, scarps along the tectonic front, and the fan morphology in the north and southeast corners of the WSB (Plate 1). Furthermore, seismic reflection profiles 102 and 105 show that the decollement lies on top of the basin fill; therefore, within the resolution of the seismic data, no tectonic accretion of trench fill sediment occurs now. Consequently, we believe that most mass wasting deposits transported to the trench are subducted.

Time Required for Shallow Deformation to Heal

Geophysical data collected in the collision zone between the NDR and the New Hebrides island arc indicate both the area of the arc slope involved in the collision and the time required for healing the morphologic disturbance that results from the collision. Although the collision of the NDR and arc might have begun far south of the Wousi Bank, the morphologic disturbance does not extend more than 20 km north and south of the ridge, as indicated by a Sea Beam map published by *Daniel et al.*, [1986]. Because the ridge is 40 km wide, the deformed area appears to be approximately twice the width of the ridge. If the DEZ has been subducting since at least 2 Ma [*Carney et al.*, 1985; *Pascal et al.*, 1978] and moved along the trench at an average rate of 2.5 cm/yr, healing of the main morphologic features of arc slope deformation appears to have been completed in about 0.8 m.y. Although this value may be affected by the uncertainty of the plate convergence direction (76°±11°E) [*Isacks et al.*, 1981], the healing time appears to be greater than that required for healing reentrants created by arc-seamount collisions along the Japan (0.6 Ma) [*von Huene and Lallemand*, 1989] and Peru (0.2 Ma) [R. von Huene, personal communication, 1989] margins.

CONCLUSION

Single-channel seismic sections and Sea Beam data collected in the collision zone between the NDR and the New Hebrides island arc indicate that although the obliquity of the NDR relative to the plate convergence is small, trench-parallel structures are poorly developed and confined to near the toe of the accretionary complex. In contrast, geophysical data demonstrate that the slow creeping of the ridge northward along the trench as well as the shape of the ridge exert a strong influence on the morphology, tectonics, and erosion of the accretionary complex in this collision zone. This influence is revealed by the development in the collision zone of three tectonically distinct parts that define a general asymmetric tectonic pattern across the arc slope. (1) In the northern part of the collision zone, accreted rocks accommodate the oblique subduction of the ridge by shortening, mass wasting, and trenchward extrusion along inferred transpressive or strike-slip faults that trend N60°W; (2) in the central part of the collision zone, vigorous uplift and local collapse occur above the subducted crest of the ridge; and (3) in the southern part of the collision zone, important mass wasting and large collapse develop along east trending faults. This accommodation occurs in a complex three-dimensional environment and depends on various parameters such as the relative variation of shear stress along the decollement and the strength of accreted rocks.

Gravity tectonics and mass wasting are important processes that shape the arc slope in a collision zone. Several mechanisms that contribute to a vigorous erosion of the arc slope were identified along this collision zone. Repeated mobilization of accreted rocks that form overlapping slides appears to be typical of mass wasting across the gentle arc slope north of the ridge; block sliding along an extensional detachment that dips through accreted rocks is believed to be evidence for denudation of the accretionary complex above the ridge; and large normal faults accompanied by numerous slump masses are shown to be characteristic of the tectonic erosion produced by relaxation of the arc slope in the wake of the ridge. The area of the collision zone that is affected by tectonic erosion and mass wasting is about twice as large as the width of the ridge and the time required to heal the morphologic disturbances caused by the ridge subduction is of the order of 0.8 m.y.

Acknowledgments. We are grateful to Jacques Récy for assistance in planning the experimental strategy. We thank Jacques Daniel, chief scientist on SEAPSO and MULTIPSO cruises for providing data from these cruises; Jack G. Vedder, Roland von Huene, and Serge Lallemand for reviewing this report; and Susan Vath for drafting.

REFERENCES

Andrews, J.E., et al., Site 286, *Initial Reports of the Deep Sea Drilling Project, 30*, p. 69-131, 1975.

Ballance, P. F., D. W. Scholl, T. L. Vallier, A. J. Stevenson, Ryan H, and R. H. Herzer, Subduction of a Late Cretaceous seamount of the Louisville Ridge at the Tonga Trench: A model of normal and accelerated tectonic erosion, *Tectonics*, 8, 953-962, 1989.

Burne, R.V., J.Y. Collot, and J. Daniel, Superficial structures and stress regimes of the downgoing plate associated with subduction-collision in the central New Hebrides arc (Vanuatu), in *Geology and Offshore Resources of Pacific Island Arcs, Vanuatu Region*, Earth Sci. Ser., vol. 8, edited by Greene, H.G. , and Wong, F.L., p 357-376, Circum Pacific Council for Energy and Mineral Resources, , Houston, Tex., 1988.

Carney , J.N.,and A. Macfarlane, A sedimentray basin in the central New Hebrides arc, *U.N. Econ. and Soc. Comm. for Asia and the Pac., Tech. Bull.* 3, 109-120, Suva, Fiji, 1980.

Carney, J.N., and A. Macfarlane, Geological evidence bearing on the Miocene to Recent structural evolution of the New Hebrides arc,*Tectonophysics*, 87, 147-175, 1982.

Carney, J.N., A. Macfarlane, and, D.I.J., Mallick, The Vanuatu island arc: an outline of the stratigraphy, structure, and petrology, in *The Ocean Basins and Margins*, vol. 7A, edited by A. E. M. Nairn, F. G. Stehli, and S. Uyeda, pp. 683-718, Plenum, New York, 1985.

Chase, C.G., Tectonic history of the Fiji Plateau, *Geol. Soc. Am. Bull.*, *82*, 3087-3109, 1971.

Chung, W.Y., and H. Kanamori, Subduction process of a fracture zone and aseismic ridges-the focal mechanism and source characteristics of the New Hebrides earthquake of 1969 January 19 and some related events, *Geophys. J. R. Astron. Soc.*, *54*, 221-240, 1978.

Collot, J. Y., and M. A. Fisher, Crustal structure from gravity data of a collision zone in the central New Hebrides island arc, in *Geology and Offshore Resources of Pacific Island Arcs-Vanuatu Region, Earth Sci. Ser.*, vol. 8 edited by H.G. Greene and F.L. Wong, pp. 125-140, Circum Pacific Council for Energy and Mineral Resources, Houston, Tex., 1988.

Collot, J.Y., J. Daniel, and R.V. Burne, Recent tectonics associated with the subduction/collision of the d'Entrecasteaux zone in the central New Hebrides, *Tectonophysics*, *112*, 325-356, 1985.

Collot, J. Y., and M. A. Fisher, Formation of forearc basins by collision

between seamounts and accretionary wedges: An example from the New Hebrides island arc, *Geology, 17*, p. 930-934, 1989.

Daniel, J., and H.R. Katz, d'Entrecasteaux zone, trench and western chain of the central New Hebrides island arc: Their significance and tectonic relationship, *GeoMar. Lett., 1*, 213-219, 1981.

Daniel, J. et al., Subduction et collisions le long de l'arc des Nouvelles-Hébrides (Vanuatu): résultats préliminaires de la campagne SEAPSO(leg 1), C. *R. Acad. Sci., 303*, 805-810, 1986.

Davis, D., J. Suppe, and F.A. Dahlen, Mechanics of fold-and-thrust belts and accretionary wedges, *J. Geophys. Res., 88*,1153-1172, 1983.

Falvey, D.A., Arc reversals, and a tectonic model for the north Fiji Basin, *Bull. Aust. Soc. Explor. Geophys. , 6*, 47-49, 1975.

Fisher, M.A., J.Y. Collot, and G.L. Smith, Possible causes for structural variation where the New Hebrides island arc and the d'Entrecasteaux zone collide, *Geology, 14*, 951-954, 1986.

Fisher, M.A., J.-Y. Collot, and E.L. Geist, The collision zone between the North d'Entrecasteaux Ridge and the New Hebrides island arc, 2, Structure from multichannel seismic data, *J. Geophys. Res.*, this issue.

Fisher, M. A., D. A. Falvey, and G.L. Smith, Seismic stratigraphy of the summit basins of the New Hebrides island arc, *in Geology and Offshore Resources of Pacific Island Arcs-Vanuatu Region, Earth Sci Ser.*, vol. 8, edited by H.G. Greene, and F.L. Wong, pp. 201-223, Circum Pacific Council for Energy and Mineral Resources, Houston, Tex., 1988.

Greene, H. G., and D. P. Johnson, Geology of the central basin region of the New Hebrides arc inferred from single-channel seismic reflection data, in *Geology and Offshore Resources of Pacific Island Arcs-Vanuatu Region,as, Earth Sci. Ser.*, vol. 8, edited by H.G. Greene and F.L. Wong, pp. 177-199, Circum Pacific Council for Energy and Mineral Resources, Houston, Tex., 1988.

Haberman, R. E., Spatial seismic variations and asperities in the New Hebrides seismic zone, *J. Geophys. Res., 89*, 5891-5903, 1984.

Isacks, B. L., R. K. Cardwell, J. L. Chatelain, M. Barazangi, J. M. Marthelot, D. Chinn, and R. Louat, Seismicity and tectonics of the central New Hebrides island arc, *in Earthquake Prediction and International review, Maurice Ewing Ser., vol. 4*, edited by D.W. Simpson and P.G. Richards, pp. 93-116, AGU, Washington, D.C., 1981.

Jouannic, C., F.W. Taylor, A.L. Bloom. and M. Bernat, Late quaternary uplift history from emerged reef terraces on Santo and Malekula Islands, central New Hebrides island arc, *Tech. Bull. 3, U.N. Econ. and Soc. Comm. for Asia and the Pac.*, pp. 91-108, Suva, Fiji,1980.

Karig, D. E., and J. Mammerickx, Tectonic framework of the New Hebrides island arc, *Mar. Geol., 12*, 187-205, 1971.

Katz, H. R., Offshore geology of Vanuatu-Previous work, in *Geology and Offshore Resources of Pacific Island Arcs-Vanuatu Region,as, Earth Sci. Ser.*, vol. 8, edited by H.G. Greene and F.L. Wong, pp. 93-122, Circum Pacific Council for Energy and Mineral Resources, Houston, Tex., 1988.

Kobayashi, K., et al., Normal faulting of the Daiichi-Kashima Samount in the Japan Trench revealed by the Kaiko I cruise, leg 3, *Earth Planet. Sci. Lett., 83*, 257-266, 1987.

Lallemand S., and X. Le Pichon, Coulomb wedge model applied to the subduction of seamonts in the Japan trench, *Geology, 15*, 1065-1069, 1987.

Lallemand, S., R. Culotta, and R. von Huene, Subduction of the Daiichi Kashima Seamount in the Japan trench, *Tectonophysics, 169*, 231-247, 1989.

Le Pichon, X.,et al., The eastern and western ends of Nankai Trough: results of Box 5 and Box 7 Kaiko survey, *Earth Planet. Sci. Lett., 83*, 199-213, 1987.

Louat, R., M. Hamburger, and M. Monzier, Shallow and intermediate depth seismicity in the New Hebrides arc: Constraints on the subduction process, in *Geology and Offshore Resources of Pacific Island Arcs-Vanuatu Region,as, Earth Sci. Ser.*, vol. 8, edited by H.G. Greene and F.L. Wong, pp.279-286, Circum Pacific Council for Energy and Mineral Resources, Houston, Tex., 1988.

Luyendyk, B. P., W. B. Bryan, and P. A. Jezek, Shallow structure of the New Hebrides island arc, *Geol. Soc. Amer. Bull., 85*, 1287-1300, 1974.

Maillet, P., M. Monzier, M. Selo, and D. Storzer, The d'Entrecasteaux zone (southwest Pacific): A petrological and geochronological reappraisal, *Mar. Geol., 53*, 179-197, 1983.

Malahoff, A., R.H., Reden, and H.S., Fleming, Magnetic anomaly and tectonic fabric of marginal basins north of New Zealand, *J. Geophys. Res., 87*, 4109-4125, 1982.

Mallick, D. I. J., Some petrological and structural variations in the New Hebrides, in *The western Pacific: Island arcs, marginal seas, geochemistry*, edited by Coleman, P. J., pp. 193-211, University of Western Australia Press, Perth, 1973.

Mallick, D.I.J., and D., Greenbaum, Geology of southern Santo, *Rep. New Hebrides Geol. Surv.*, 84 pp., 1977.

Marthelot, J.M., J.L. Chatelain, B.L. Isacks, R.K. Cardwell, and E. Coudert, Seismicity and attenuation in the central Vanuatu (New Hebrides) Islands: A new interpretation of the effect of subduction of the d'Entrecasteaux fracture zone, *J. Geophys. Res., 90*, 8641-8650, 1985.

Mitchell, A.H.G., and, A.J. Warden, Geologic evolution of the New Hebrides island arc, *J. Geol. Soc. London, 127*, 501-529, 1971.

Minster, J. B., and T. H. Jordan, Present-day plate motions, *J. Geophys. Res., 83*, 5331-5354, 1978.

Pascal, G., B.L. Isacks, M. Barazangi, and J. Dubois, Precise relocations of earthquakes and seismotectonics of the New Hebrides island arc, *J. Geophys. Res., 83*, 4957-4973, 1978.

Pelletier B., and J. Dupont, Tectonic erosion and consequent retreats of the trench and active volcanic arc due to the Louisville ridge subduction in the Tonga-Kermadec trench, *Oceanol. Acta*, in press, 1990.

Pontoise, B., and D. Tiffin, Seismic refraction results over d'Entrecasteaux Zone west of the New Hebrides arc, *Géodynamique, 1*, 109-120, 1986.

Pontoise, B. et al., La subduction de la ride de Louiseville le long de la fosse des Tonga: premiers résultats de la campagne SEAPSO (leg V), *C. R. Acad. Sci., 303*, 911-918, 1986.

Robinson, G.P., The geology of North Santo, *Rep.New Hebrides Geol. Surv.*, pp.1-77, 1969.

Saltus, R.W., and R.J. Blakeley, Hypermag: An interactive, two dimensional gravity and magnetic modeling program, *U.S. Geol. Surv. Open File Rept. 83-271*, pp. 1-31, 1983.

Tapponnier, P., and P. Molnar, Slip-line field theory and large-scale continental tectonics, *Nature,, 264*, 319-324, 1976.

Taylor, F.W., B.L. Isacks, C. Jouannic, A.L. Bloom, and J. Dubois, Coseismic and Quaternary vertical tectonic movements, Santo and Malekula Islands, New Hebrides island arc, *J. Geophys. Res., 85*, 5367-5381, 1980.

Taylor, F.W., C. Jouannic, and A.L. Bloom, Quaternary uplift of the Torrres Islands, northern New Hebrides frontal arc: Comparison with Santo and Malekula Islands, central New Hebrides arc, *J. Geol., 93*, 419-438, 1985.

Taylor, F. W., C. Frolich, J. Lecolle, and M. Strecker, Analysis of partially emerged corals and reef terraces in the central Vanuatu arc: Comparison of contemporary coseismic and nonseismic with Quaternary vertical movements, *J. Geophys. Res., 92*, 4905-4933, 1987.

von Huene, R., and S. Lallemand, Tectonic erosion along the Japan and Peru convergent margins, Geological Society of America Bulletin, *102*, 704-720, 1990.

Weissel, J K, A. B. Watts and A. Lapouille, Evidence for late Paleocene to late Eocene seafloor in the southern New Hebrides basin, *Tectonophysics., 87*, 243-251, 1983.

J.-Y. Collot, ORSTOM, Laboratoire de Geodynamique, B.P. 48, 06230 Villefranche s/mer, France.

M.A. Fisher, U.S. Geological Survey, MS 999, 345 Middlefield Road, Menlo Park, CA 94025

(Received May 2, 1989;
revised March 12, 1990;
accepted August 24, 1990)